

Jenny Stavrakou, Royal Belgian Institute for Space Aeronomy (BIRA-IASB)

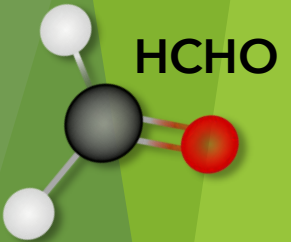
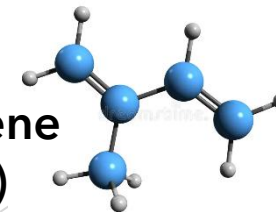
# Inversion of sources and application to pyrogenic emissions and organic aerosol precursors



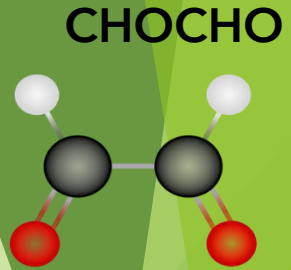
# Outline

- ✓ What is the source inversion?
- ✓ Cost function
- ✓ Minimization
- ✓ How to solve source inversion problems...
  - idealized examples
  - real atmosphere
- ✓ Why VOCs matter?
- ✓ From HCHO to VOCs : an example from the real atmosphere
- ✓ Satellite observations of HCHO
- ✓ Top-down VOC emissions from pyrogenic and biogenic sources
- ✓ Satellite-based trends

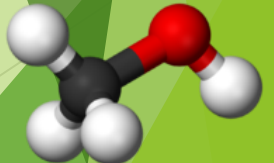
Isoprene  
(C<sub>5</sub>H<sub>8</sub>)



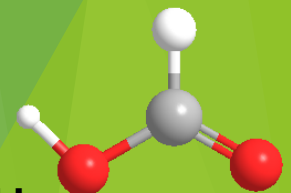
HCHO



CHOCHO

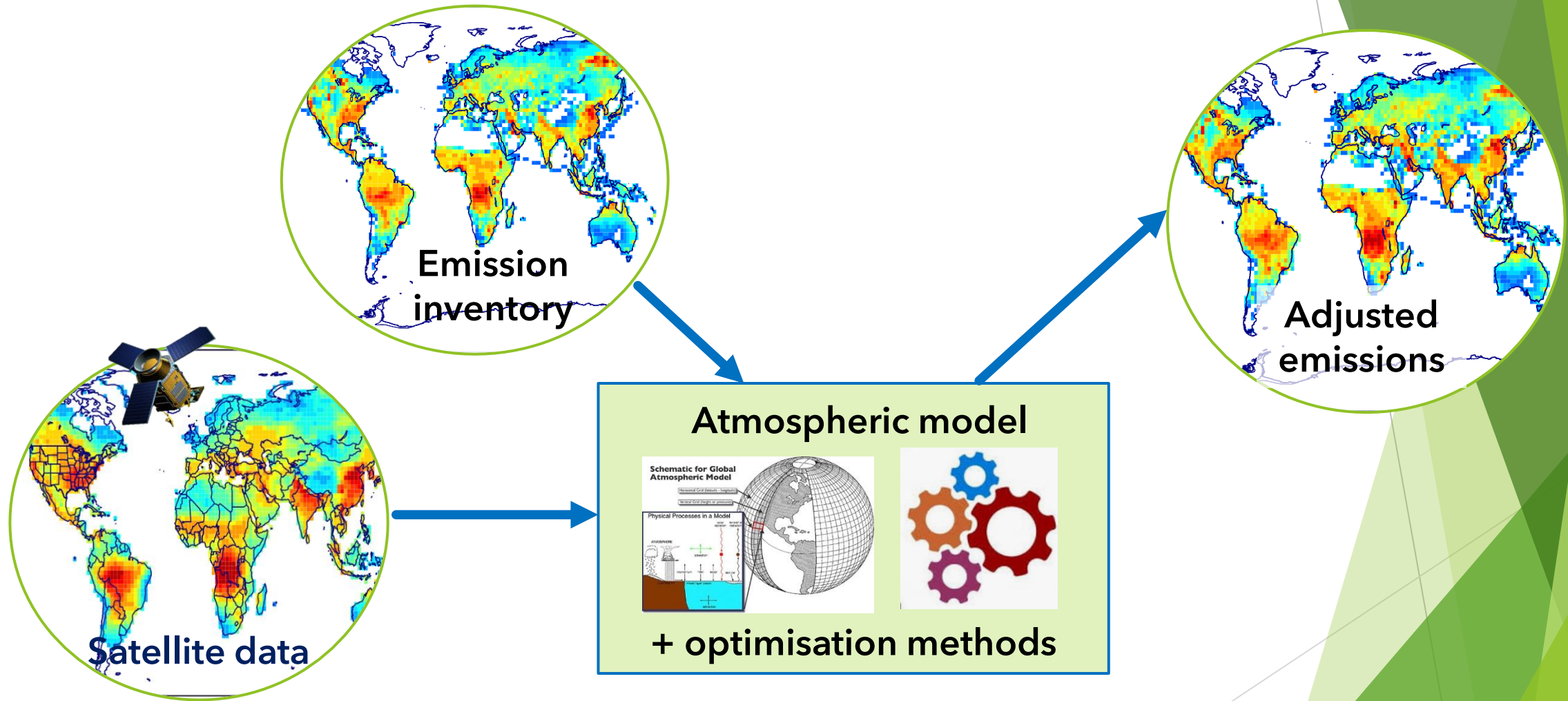


CH<sub>3</sub>OH



HCOOH

# In the nutshell: source inversion uses observations to determine emissions





**Ground-based:** Offers continuous time series of species (in situ or column) at fixed locations



**Sonde:** Supplies in situ vertical profiles through the atmosphere

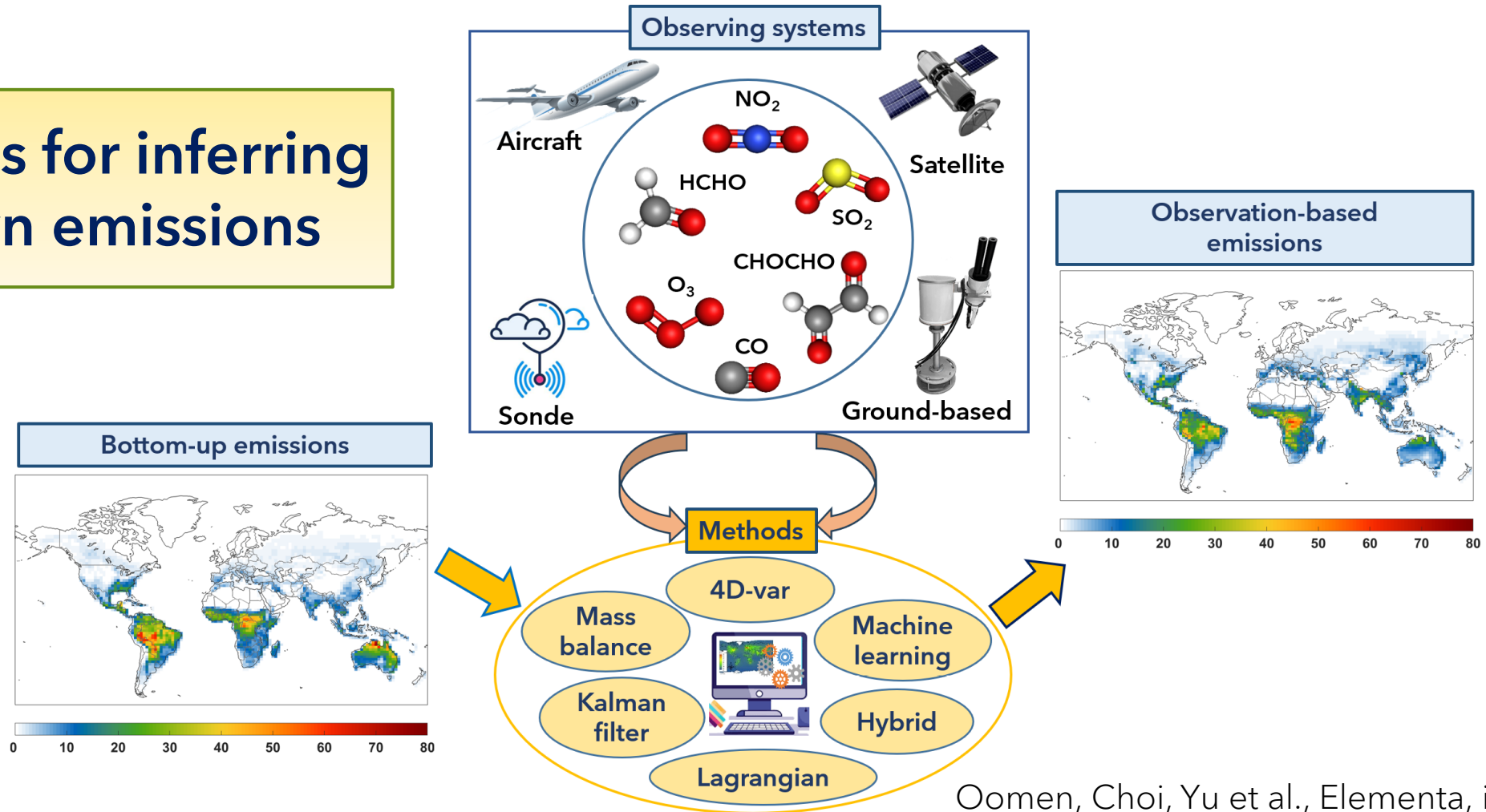


**Aircraft:** Captures atmospheric composition across altitude ranges during campaigns.



**Satellite:** Provides columns of trace gases over wide areas and extended periods. e.g. OMI, TROPOMI, CrIS, TES, GEMS, TEMPO, Sentinel-4

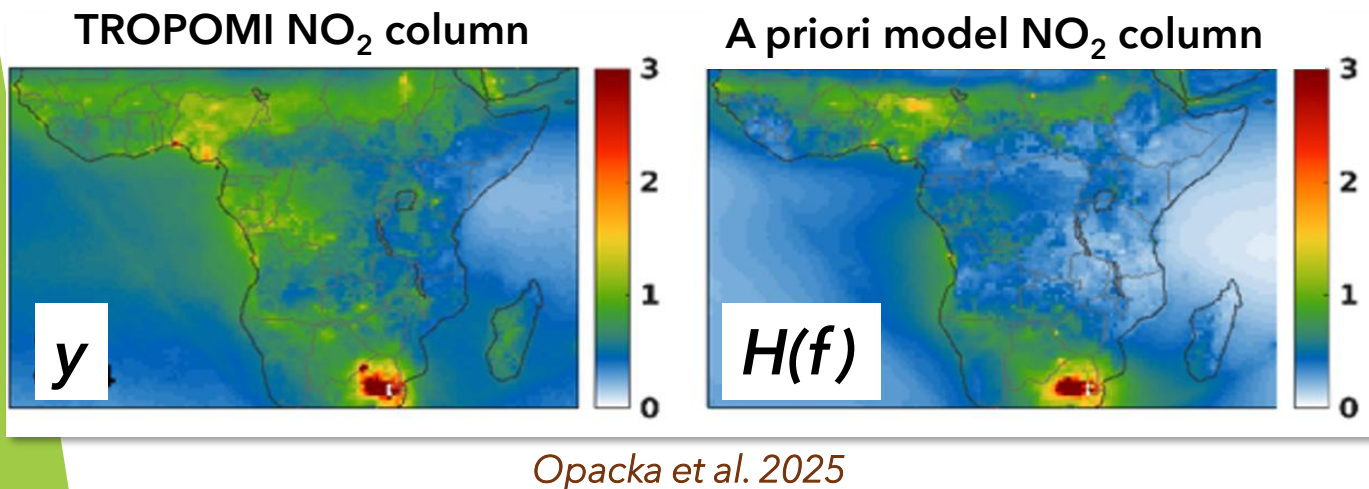
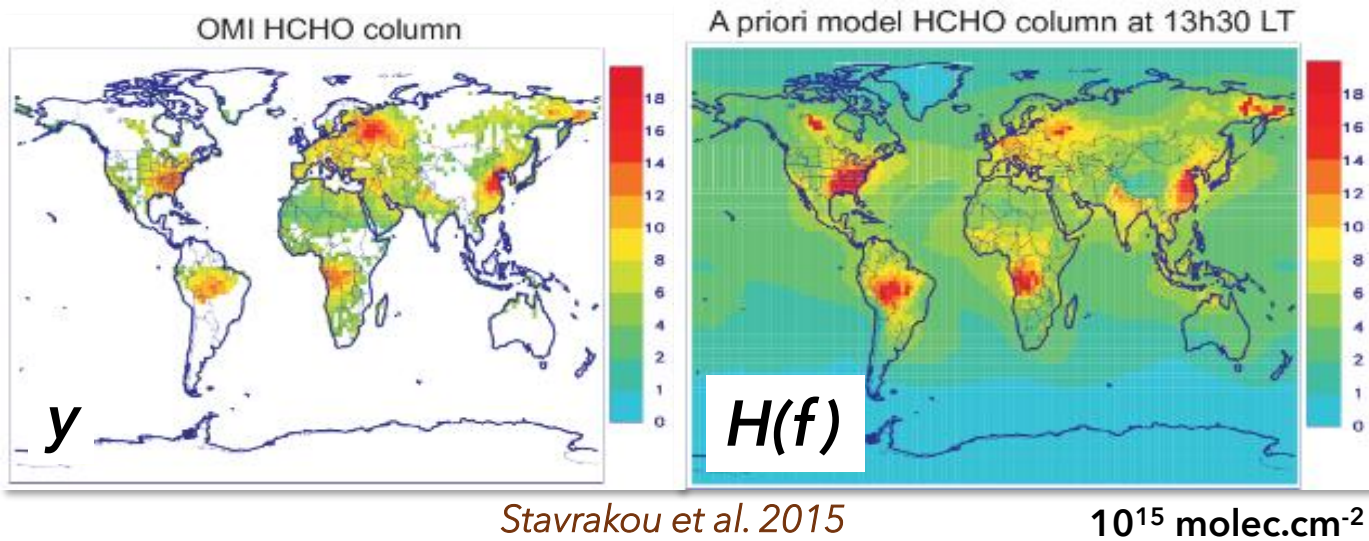
# Ingredients for inferring top-down emissions



Oomen, Choi, Yu et al., Elementa, in review



# Cost function $J$ : measure of the mismatch between model and data



A priori emission distributions

$$G_0(x, t) = \sum_{j=1}^m \Phi_j(x, t)$$

Optimised emission distributions

$$G(x, t) = \sum_{j=1}^m \exp(f_j) \cdot \Phi_j(x, t)$$

$$J(f) = J_{\text{OBS}}(f) + J_B(f)$$
$$= \frac{1}{2} \left[ (H(f) - y)^T E^{-1} (H(f) - y) + f^T B^{-1} f \right]$$

$f$  = parameters to be optimized

$f_B$  = first guess value for control parameters

$y$  = atmospheric observations

$E$  = matrix of errors on observations

$B$  = matrix of errors on a priori fluxes

Adjust emission distributions to best reproduce the observations



# Minimum of the cost function?

The cost function  $J$  is an example of complex numerical algorithm consisting in a composition of differentiable mappings



$$\begin{aligned} J(f) &= J_{obs}(f) + J_B(f) \\ &= \frac{1}{2} \sum_{i=1}^p (H_i(f) - y_i)^T \mathbf{E}^{-1} (H_i(f) - y_i) \\ &\quad + \frac{1}{2} (f - f_B)^T \mathbf{B}^{-1} (f - f_B), \end{aligned}$$

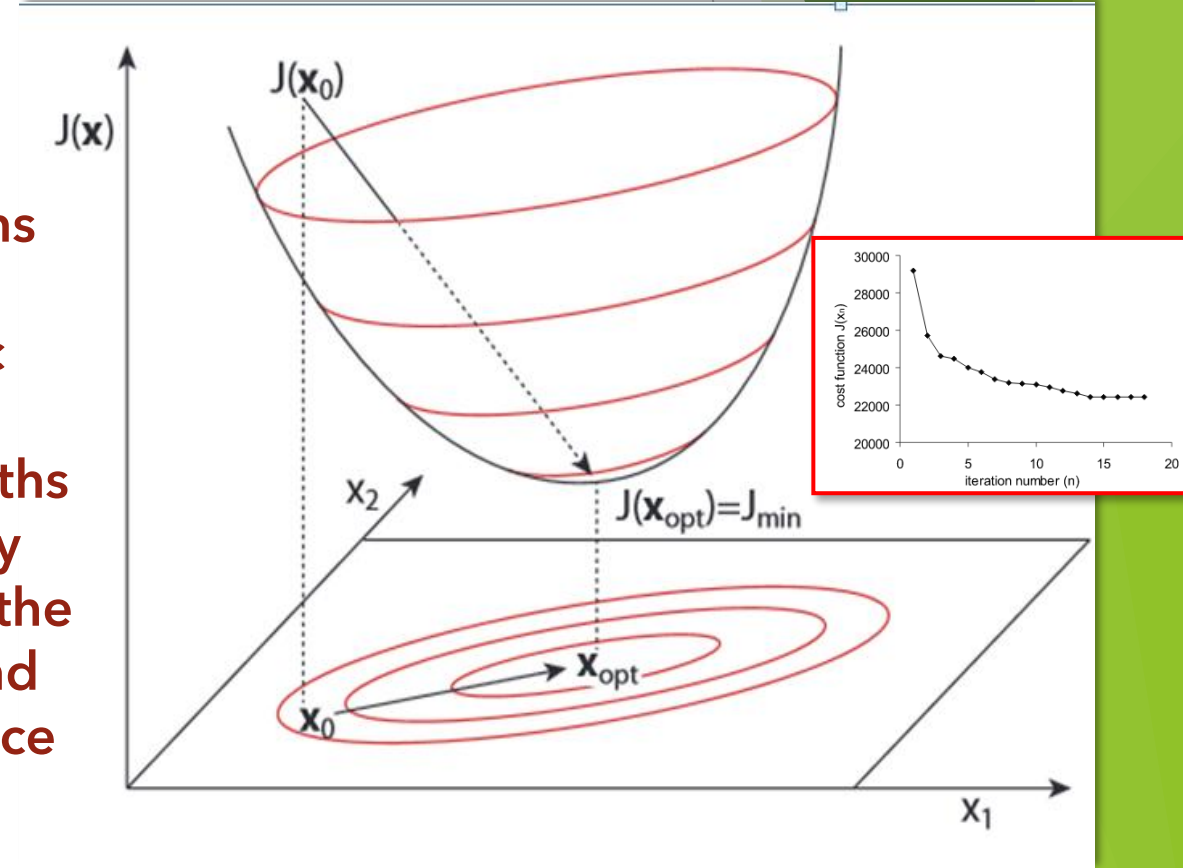


$$\begin{aligned} (\nabla J)_f &= \sum_{i=1}^p (DH_i)_f^T \mathbf{E}^{-1} (H_i(f) - y_i) \\ &\quad + \mathbf{B}^{-1} (f - f_B) \end{aligned}$$

Minimum ? Gradient of  $J=0$

Example of cost function defined in a 2d-parameter space

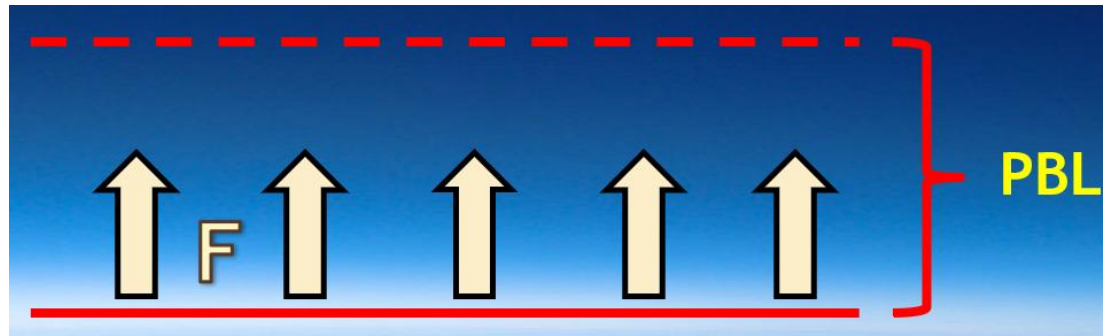
$J(\mathbf{x})$  projections on parameter plane: elliptic iso-cost lines with axis lengths determined by  $\text{grad}J$  and by the uncertainty and error covariance of  $\mathbf{x}_{\text{opt}}$



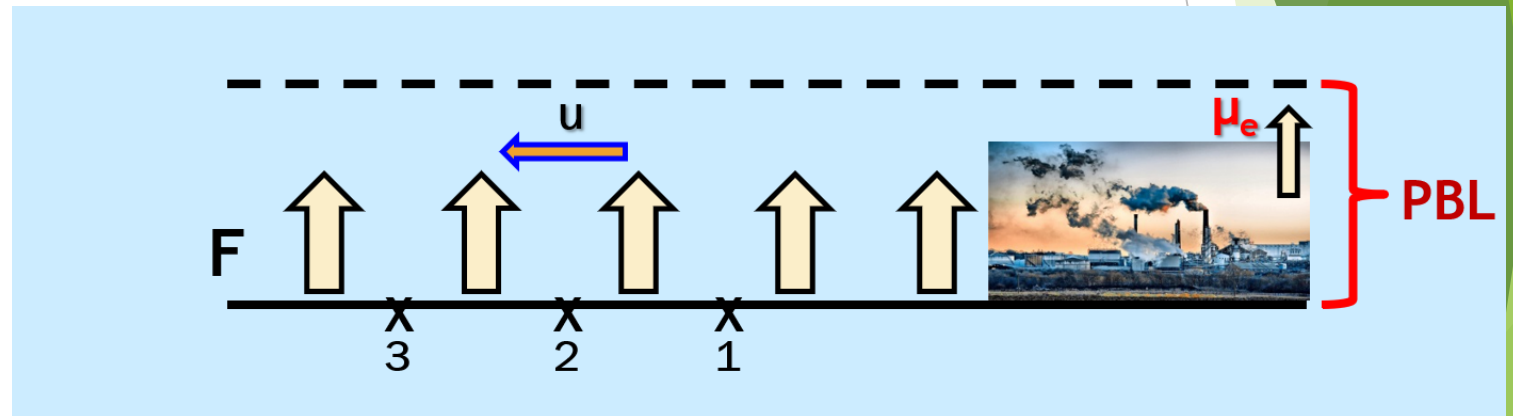


# Learning how to solve an inversion problem!

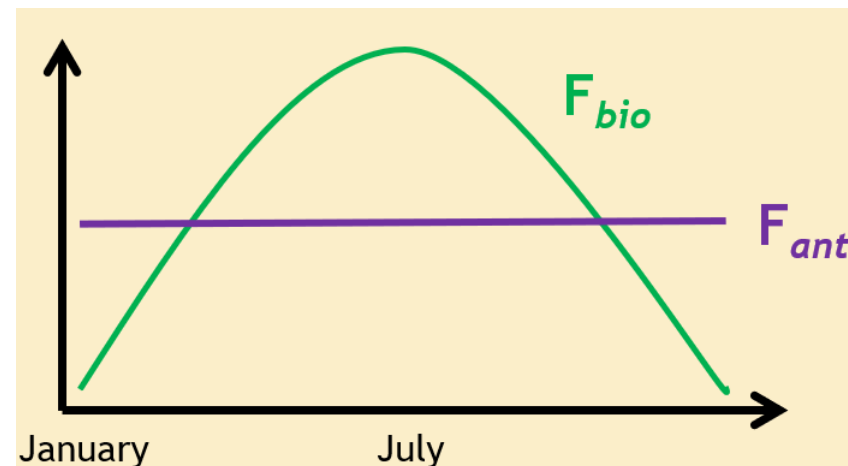
- ✓ No transport, constant sink, 1 source



- ✓ Transport, constant sink, 2 sources

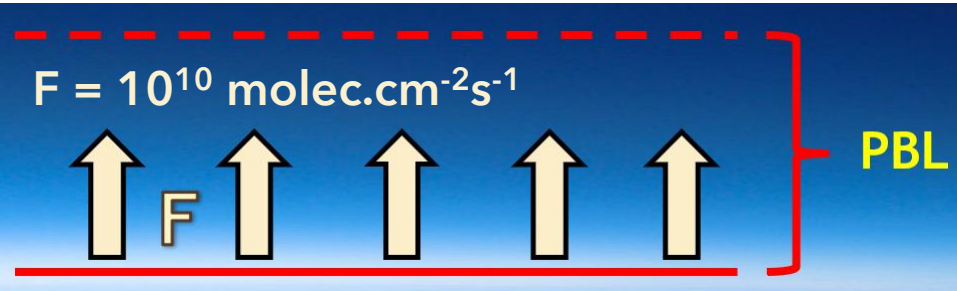


- ✓ Seasonal variation of emission sources, 2 sources





# The simplest source inversion problem: *No transport, constant sink, 1 source*



- Uniform flux  $F$  of compound A
- $A + OH \rightarrow$  rate  $k=10^{-11} \text{ molec}^{-1}\text{cm}^3 \text{ s}^{-1}$ ,  $[OH]=10^6 \text{ molec.cm}^{-3}$
- PBL : assumed well-mixed at all times ( $z=10^5 \text{ cm}$ )
- Air number density ( $n$ ) is constant ( $n=2.5 \times 10^{19} \text{ molec.cm}^{-3}$ )

## Forward problem :

- What is the resulting vertical column  $V$  of A ?
- What is the average mixing ratio ( $\mu$ )?

$$V = F / (k \cdot [OH]) \rightarrow V = 10^{15} \text{ molec.cm}^{-2}$$

$$\mu = V / n \cdot z \rightarrow \mu = 400 \text{ pptv}$$

- 3 measurements  $\mu^1_o=450 \text{ pptv}$ ,  $\mu^2_o=390 \text{ pptv}$ ,  $\mu^3_o=330 \text{ pptv}$ ,  $\Delta\mu_o = 20 \text{ pptv}$
- A priori flux estimate :  $F_o = 5 \times 10^9 \text{ molec.cm}^{-2}\text{s}^{-1}$ , uncertainty=100%
- Uncertainties in  $n$ ,  $z$ ,  $k$  and  $[OH]$  lead to additional uncertainty on modelled mixing ratio of  $\Delta\mu_m=50 \text{ pptv}$

## Inverse problem :

What is the top-down flux  $F$ ?

- A priori mixing ratio :  $\mu_o = F_o / n \cdot z \cdot k \cdot [OH] = 200 \text{ pptv}$
- Set:  $F = F_o \cdot f$ ,  $f$  = dimensionless adjustable parameter

$$J = \frac{1}{2} \sum_1^3 \left( \frac{\mu_{\text{mod}}(f) - \mu_o^i}{\Delta\mu} \right)^2 + \frac{1}{2} \left( \frac{f - f_0}{\Delta f} \right)^2$$

$$f_0 = 1$$

$$\Delta f = 1 (=100\%)$$

$$(\Delta\mu)^2 = (\Delta\mu_o)^2 + (\Delta\mu_m)^2 = (20^2 + 50^2) \text{ pptv}^2$$

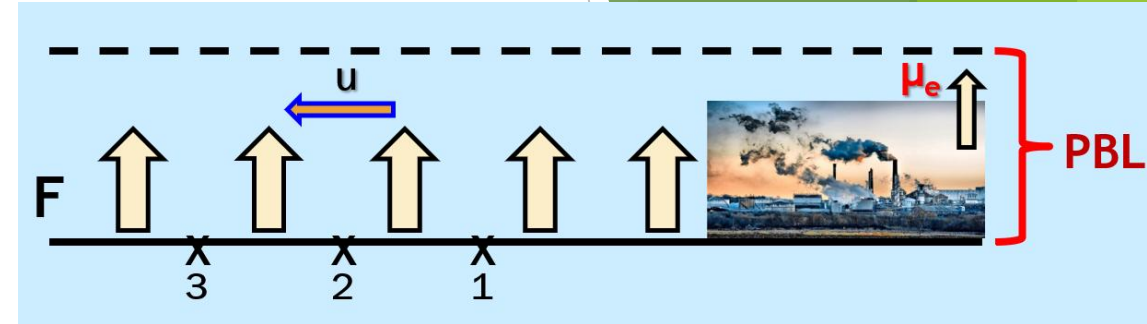
$$\frac{\partial J}{\partial f} = \frac{200}{\Delta\mu^2} \sum_1^3 200 \cdot (200 \cdot f - \mu_o^i) + (f - 1) = 0 \Rightarrow f = 1.927$$

$$F = F_o \cdot f = 9.64 \times 10^9 \text{ molec.cm}^{-2}\text{s}^{-1}$$

Very close to the true flux!

# A bit more complicated: *Constant transport, constant sink, 2 sources to retrieve*

- Background source  $F=10^{10}$  molec.cm<sup>-2</sup>s<sup>-1</sup> + local source generating an enhancement  $\mu_e=1$  ppbv of compound A
- Constant horizontal wind :  $u = 5$  m/s
- Measurements at sites 1,2,3 downwind, at  $d_1=200$  km,  $d_2=500$  km and  $d_3=1000$  km



Forward problem: What is the mixing ratio ( $\mu$ ) at each site?

- $\mu = \mu_b + \mu_e$ , with  $\mu_b = F / (n \cdot z \cdot k \cdot [\text{OH}]) = 400$  pptv (as before)
- $\mu_e = 1 \text{ ppbv} \cdot e^{-(d/u) \cdot k \cdot [\text{OH}]} \rightarrow \mu_e(1) = 670 \text{ pptv}, \mu_e(2) = 368 \text{ pptv}, \mu_e(3) = 135 \text{ pptv}$

$$\begin{aligned} \mu(1) &= 1070 \text{ pptv} \\ \mu(2) &= 768 \text{ pptv} \\ \mu(3) &= 535 \text{ pptv} \end{aligned}$$

- ✓ Assume :  $\mu^1_o=1100$  pptv,  $\mu^2_o=750$  pptv,  $\mu^3_o=500$  ppt
- ✓ Combined measurement/model uncertainty :  $\Delta\mu=100$  pptv
- ✓  $F_o = 5 \times 10^9$  molec.cm<sup>-2</sup>s<sup>-1</sup>, uncertainty=100%
- ✓ A priori mixing ratio enhancement :  $\mu_{eo} = 2$  ppbv, 100% error

$$F = F_o \cdot f_1, \mu_e = \mu_{eo} \cdot f_2 \text{ with a priori } f_1 = f_2 = 1, \Delta f_1 = \Delta f_2 = 1$$

$$\begin{aligned} \mu^i_{\text{mod}}(f) &= (F_o \cdot f_1 / (n \cdot z \cdot k \cdot [\text{OH}])) + (\mu_{eo} \cdot f_2 \cdot e^{-(d_i/u) \cdot k \cdot [\text{OH}]}) \Rightarrow \\ \mu^1_{\text{mod}} &= 200 \cdot f_1 + 1340 \cdot f_2 \\ \mu^2_{\text{mod}} &= 200 \cdot f_1 + 736 \cdot f_2 \\ \mu^3_{\text{mod}} &= 200 \cdot f_1 + 270 \cdot f_2 \end{aligned}$$

Inverse problem :  
What are the flux  $F$  and mixing ratio  $\mu_e$ ?

$$J = \frac{1}{2} \sum_1^3 \left( \frac{\mu_{\text{mod}}(f) - \mu_o^i}{\Delta\mu} \right)^2 + \frac{1}{2} \left( \frac{f_1 - f_0}{\Delta f_1} \right)^2 + \frac{1}{2} \left( \frac{f_2 - f_0}{\Delta f_2} \right)^2$$

$$\frac{\partial J}{\partial f_1} = \frac{\partial J}{\partial f_2} = 0 \Rightarrow f_1 = 1.515, f_2 = 0.603$$

$$F = 7.575 \times 10^9 \text{ molec.cm}^{-2} \text{ s}^{-1} \& \mu_e = 1.206 \text{ ppbv}$$

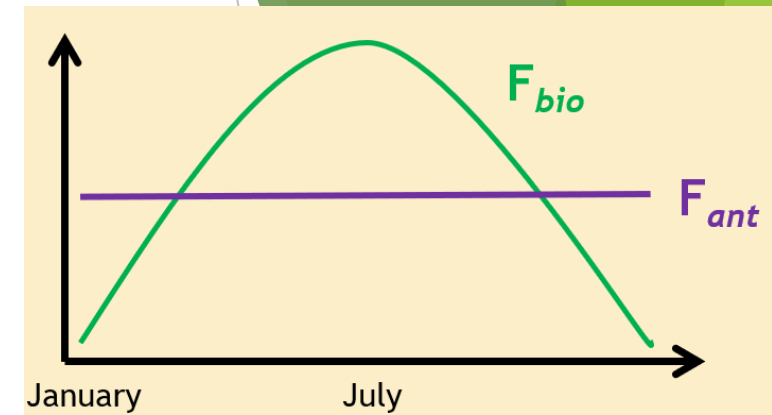


# One step further : *Retrieve 2 sources with different seasonality*

- Compound A has a constant anthropogenic source ( $F_{ant}$ ), and a biogenic source ( $F_{bio}$ ) with a seasonality peaking in summer

- $F_{ant} = 10^{10} \text{ molec.cm}^{-2}\text{s}^{-1}$
- $F_{bio}(\text{spring}) = 10^{10} \text{ molec.cm}^{-2}\text{s}^{-1}$
- $F_{bio}(\text{summer}) = 3 \times 10^{10} \text{ molec.cm}^{-2}\text{s}^{-1}$

- $\mu(\text{spring}) = (F_{ant} + F_{bio}(\text{spring})) / (n \cdot z \cdot k \cdot [\text{OH}]) = 0.8 \text{ ppbv}$
- $\mu(\text{summer}) = (F_{ant} + F_{bio}(\text{summer})) / (n \cdot z \cdot k \cdot [\text{OH}]) = 1.6 \text{ ppbv}$



- Assume  $\mu^1_o = 0.8 \text{ ppbv}$  in spring,  $\mu^2_o = 1.6 \text{ ppbv}$  in summer,  $\Delta\mu = 0.2 \text{ ppbv}$
- No correlation btw anthropogenic and biogenic source
- Correlation btw errors on biogenic source in spring and summer

**Inverse problem :**  
What is the top-down flux  $F_{ant}$  and  $F_{bio}$  ?

- $F_{ant} = 2 \times 10^{10} \cdot f_1$ ,  $F_{bio}(\text{spring}) = 10^{10} \cdot f_2$ ,  $F_{bio}(\text{summer}) = 2 \times 10^{10} \cdot f_3$  with  $f_1 = f_2 = f_3 = 1$ ,  $\Delta f_1 = 1$ ,  $\Delta f_2 = \Delta f_3 = 2/\sqrt{3}$
- Correlation between  $f_2$  and  $f_3$  is  $c=0.5$

$$J = \frac{1}{2} \sum_i \left( \frac{\mu_{\text{mod}}(f) - \mu_o^i}{\Delta\mu} \right)^2 + \frac{1}{2} \sum_{j=1}^3 \sum_{k=1}^3 (f_j - 1) B_{jk}^{-1} (f_k - 1)$$

$$\begin{pmatrix} \Delta f_1^2 & 0 & 0 \\ 0 & \Delta f_2^2 & c \Delta f_2 \Delta f_3 \\ 0 & c \Delta f_2 \Delta f_3 & \Delta f_3^2 \end{pmatrix}$$

$$\frac{\partial J}{\partial f_1} = \frac{\partial J}{\partial f_2} = \frac{\partial J}{\partial f_3} = 0 \Rightarrow f_1 = 0.66, f_2 = 0.76, f_3 = 1.31$$

$$F_{ant} = 1.33 \times 10^{10}, F_{bio}(\text{spring}) = 0.76 \times 10^{10}, F_{bio}(\text{summer}) = 2.6 \times 10^{10}$$

$$\mu^1_{\text{mod}} = 0.839 \text{ ppbv}, \mu^2_{\text{mod}} = 1.579 \text{ ppbv}$$

Very close to the real values!

## And in the real atmosphere?

Same formula!

$$J = \frac{1}{2}(H(f) - y)^T E^{-1}(H(f) - y) + \frac{1}{2}(f - f_B)^T B^{-1}(f - f_B)$$

- $y$  : chemical observations from satellite, ground-based, airborne...
- $H(f)$  : global or regional CTM
- $E$  : errors of the retrievals (systematic/random)
- $B$  : based on spatiotemporal correlations

In numbers...

- Global CTM (2°x2.5°, 144 longitudes x 90 latitudes)
- Optimize monthly fluxes of compound A
- 3 emission sources (e.g. biogenic, pyrogenic, anthropogenic)
- #  $f$ 's :  $12 \times 144 \times 90 \times 3 \times 0.3 \sim 140,000$  parameters to optimize

Even when we use satellite measurements to constrain the fluxes, we have fewer observations ( $12 \times 144 \times 90 \times 0.3 \sim 50,000$ ) than parameters to optimize → *Underdetermined problem*



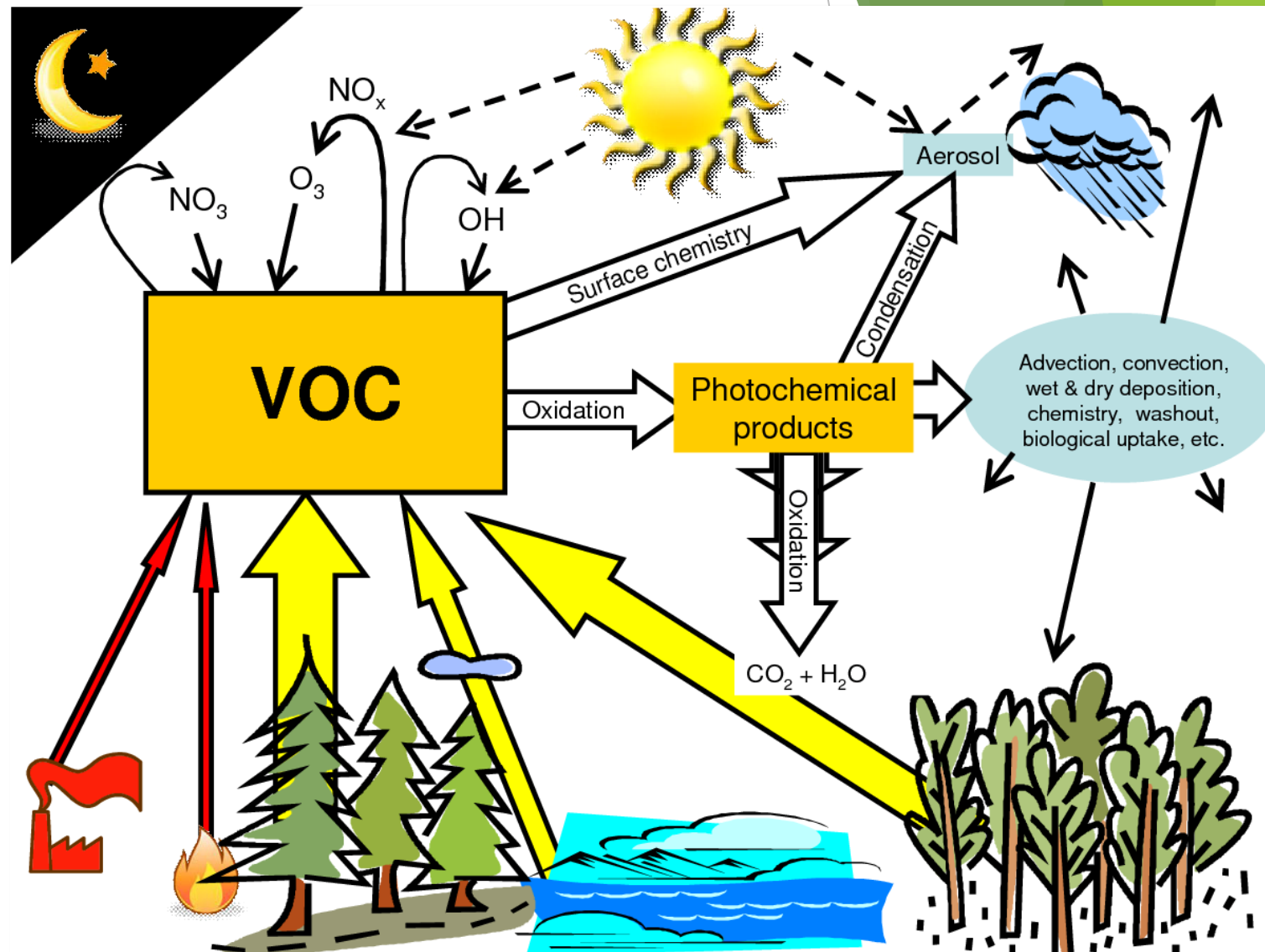
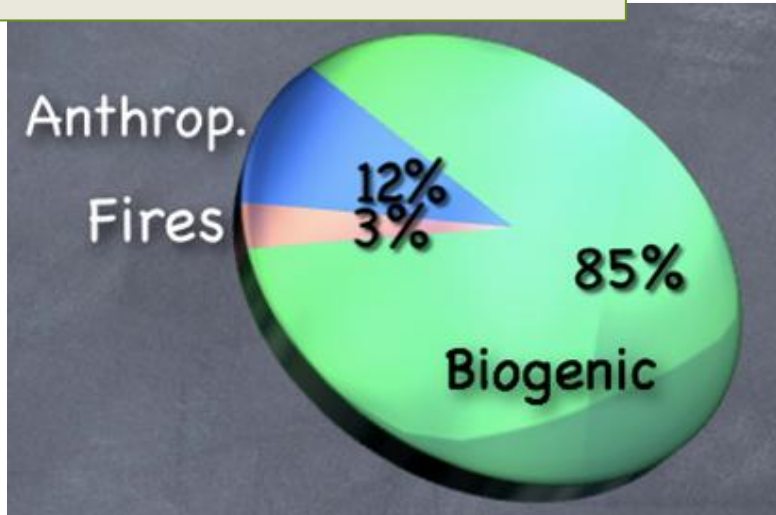
Reduce the number of effective variables by omitting cells with very low a priori flux, and by using a correlation setup in matrix  $B$



# NMVOCs : why do they matter?

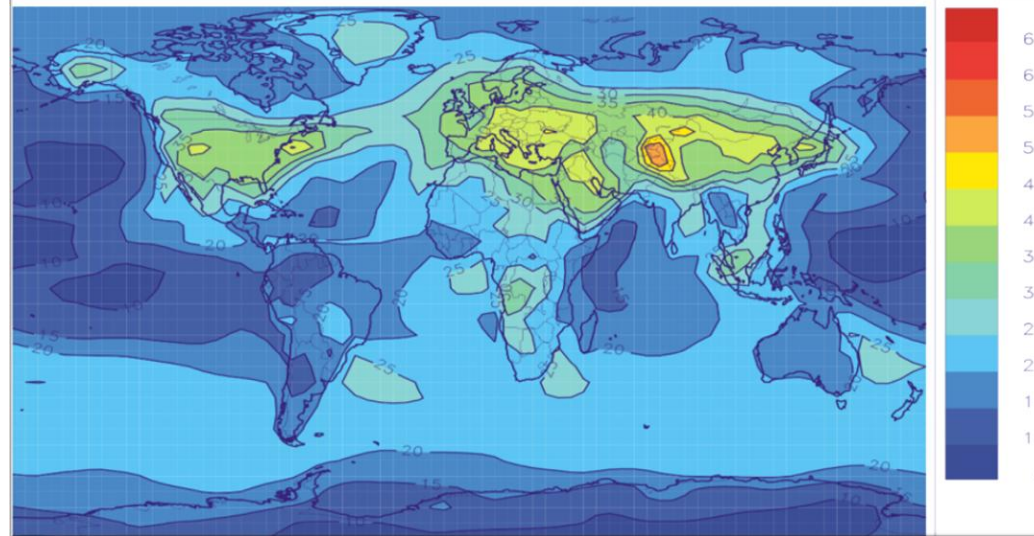
- Broad variety of fast reacting species
- Influence atmospheric composition : contribute to  $O_3$  & PM formation
- Influence radiation, clouds, air quality
- Influence human health & climate : precursors of SOA, affect GHG

Annual emission : ~1000 TgC (isoprene~500 TgC), but large uncertainties!

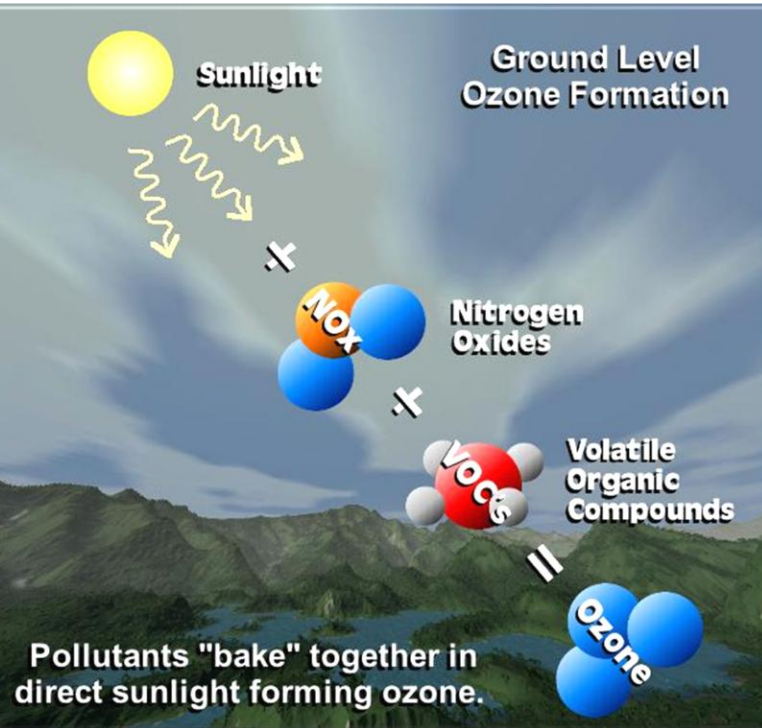
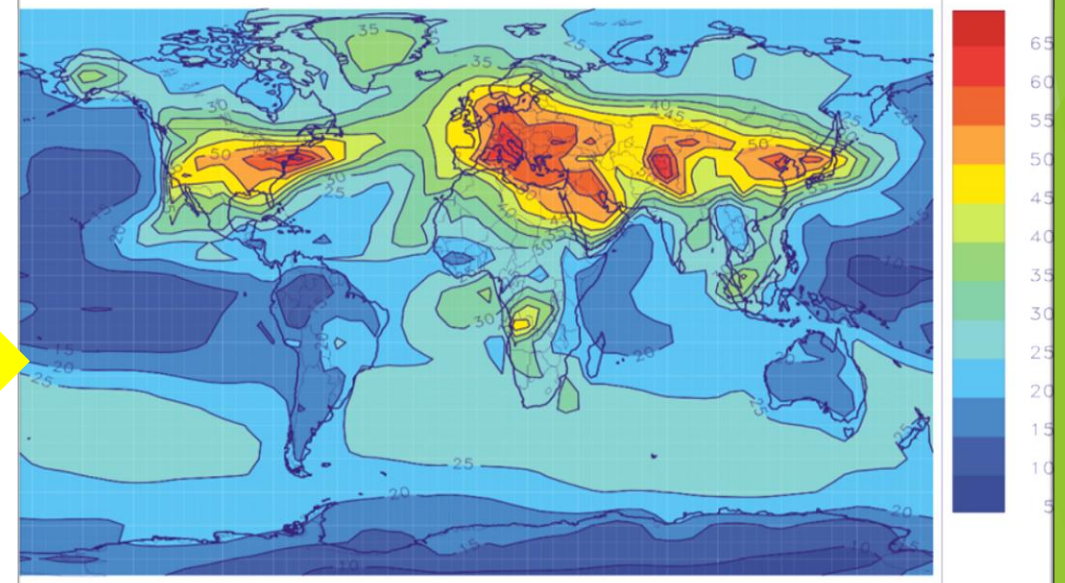


# Impact of NMVOC precursors on surface ozone levels

Model simulation neglecting NMVOCs



Model simulation with NMVOCs

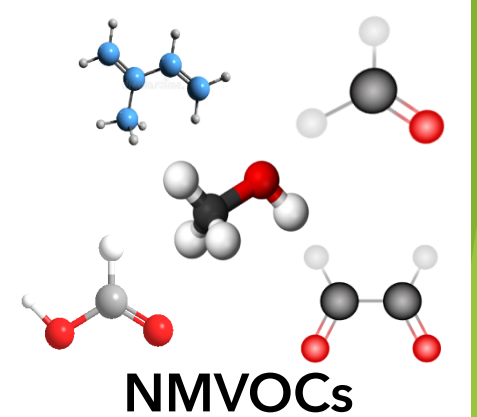
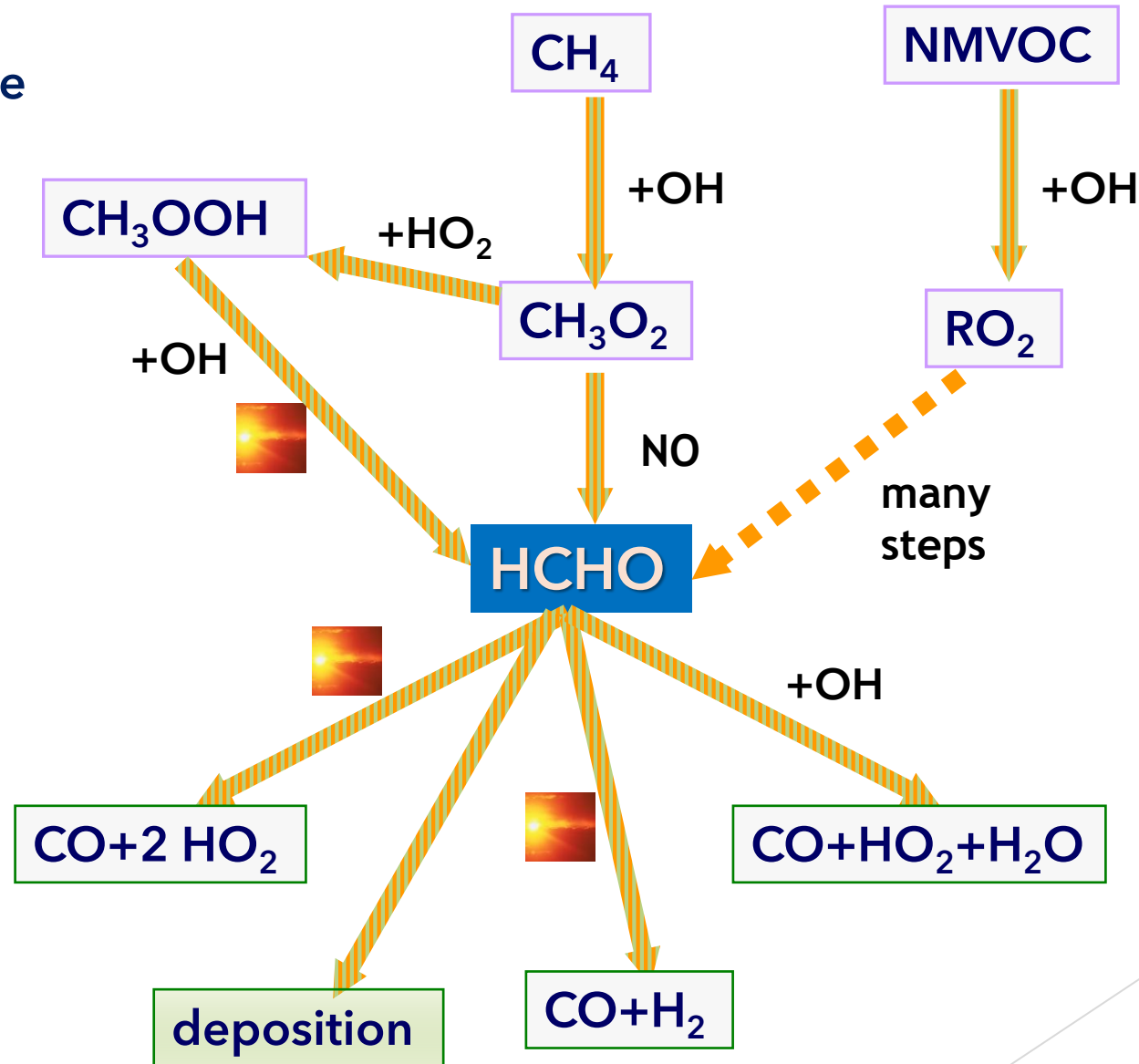


In the presence of VOCs → strong increases of surface ozone levels in the Northern Hemisphere, up to factor of 2 increase in eastern US, Europe and China



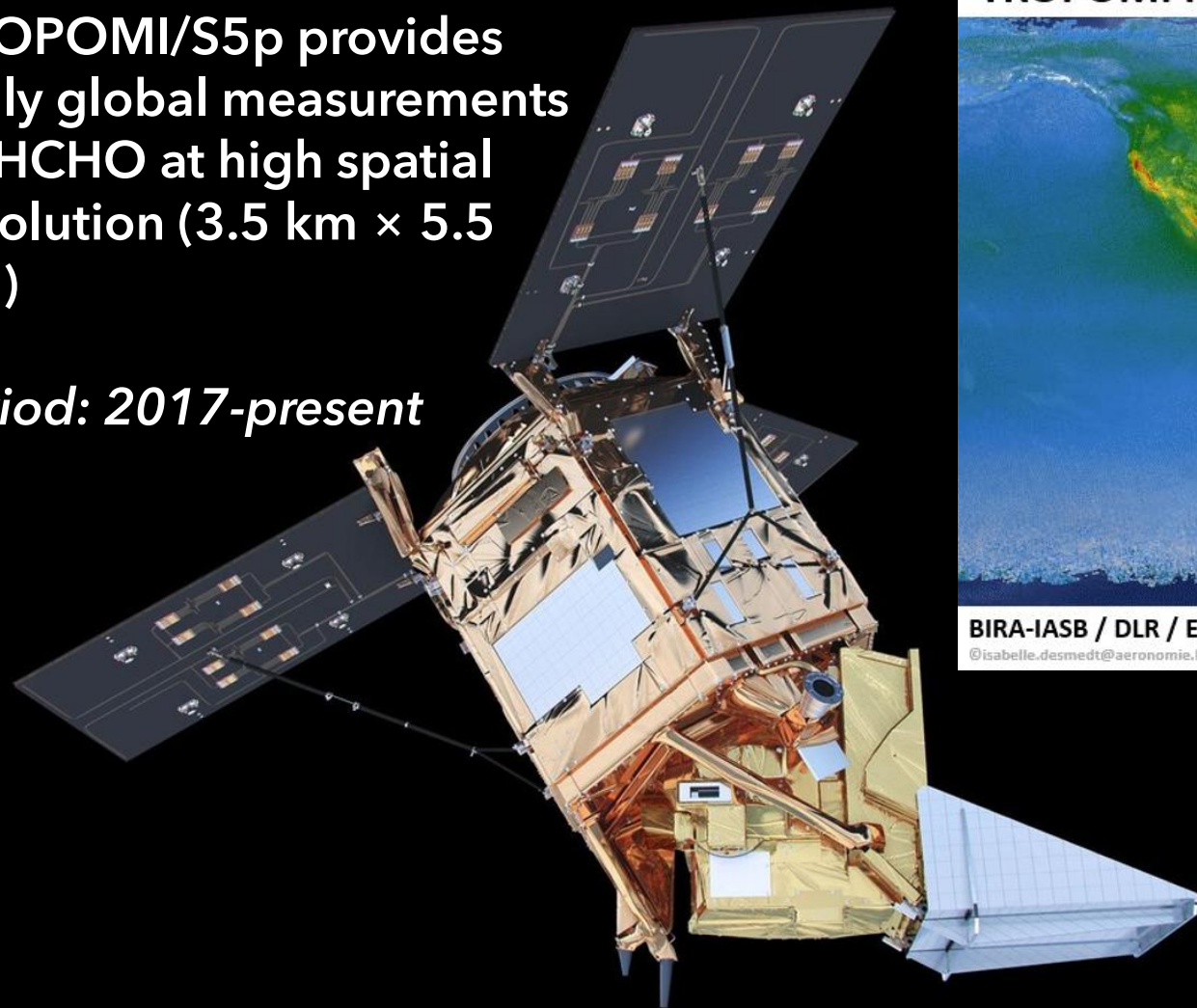
# HCHO : the most abundant carbonyl in the atmosphere

- ✓ Short-lived - lifetime on the order of a few hours
- ✓ Directly emitted from fossil fuel combustion and biomass burning
- ✓ Also formed as a high-yield secondary product in the  $\text{CH}_4$  and NMVOC oxidation



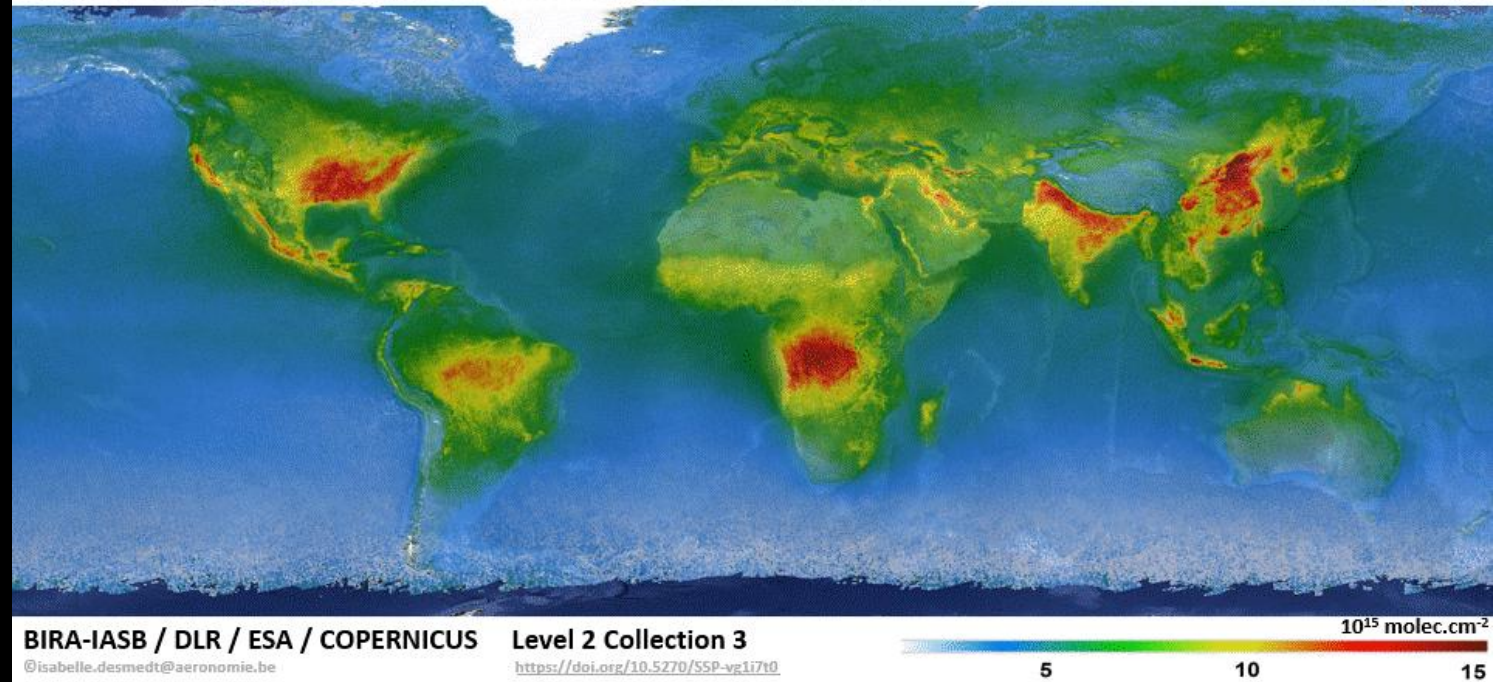
TROPOMI/S5p provides daily global measurements of HCHO at high spatial resolution (3.5 km × 5.5 km)

*Period: 2017-present*



TROPOMI HCHO TROPOSPHERIC COLUMNS

JJA 2018



Infer top-down

- pyrogenic VOC emissions
- biogenic VOC emissions

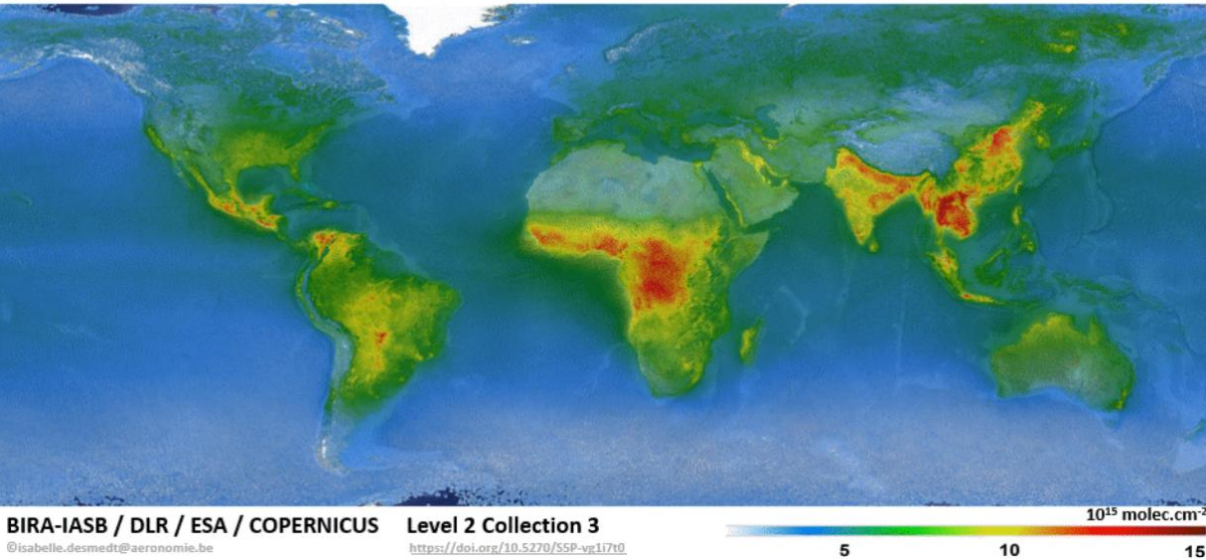
*based on MAGRITTE global CTM and its adjoint (4D-Var)*



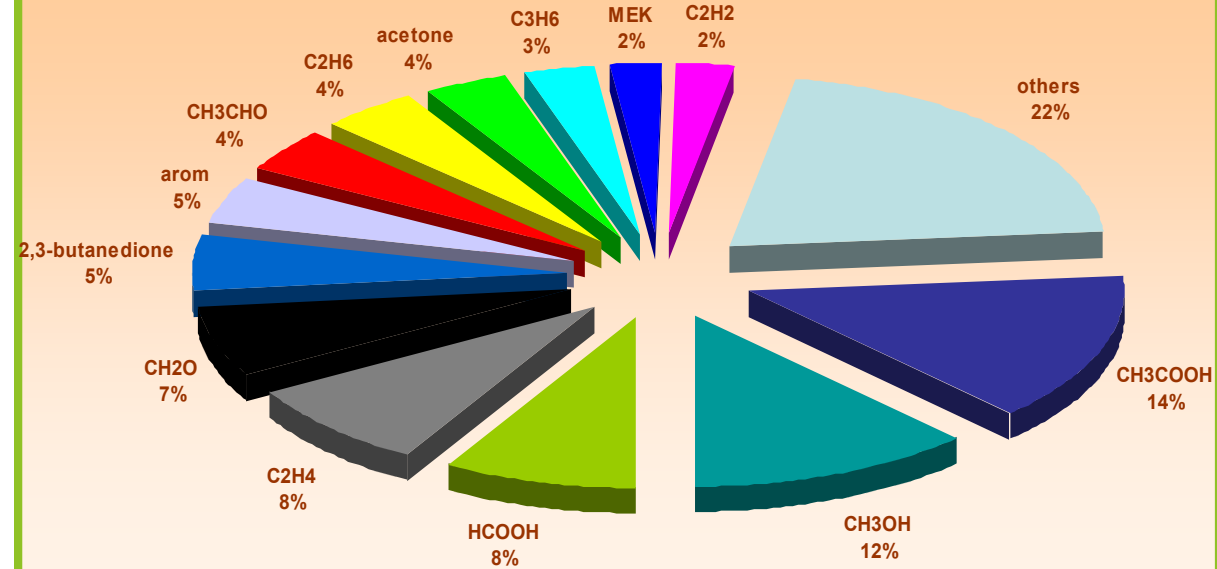
# Focus on pyrogenic and biogenic sources

TROPOMI HCHO TROPOSPHERIC COLUMNS

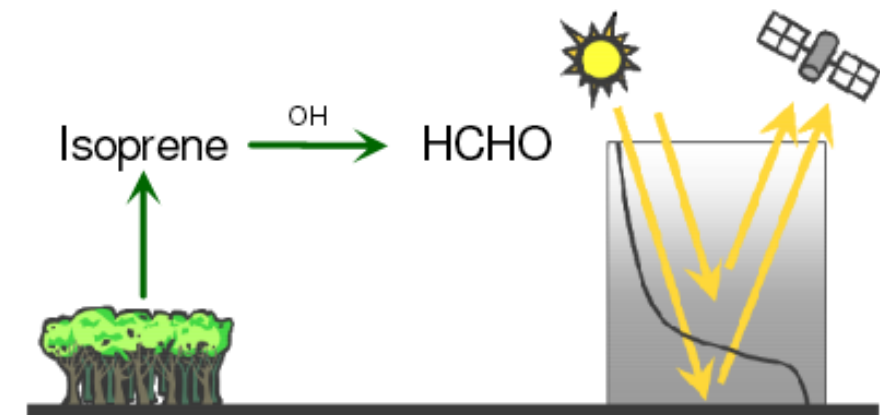
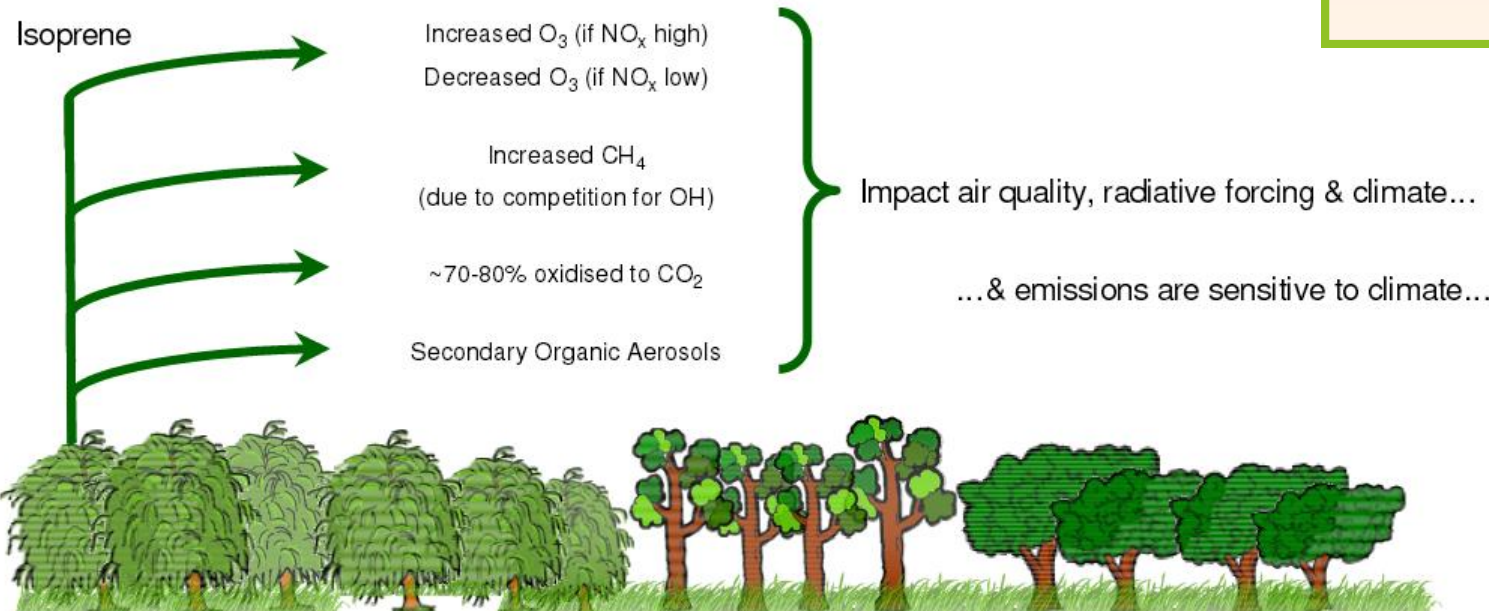
JJA 2020



NMVOC emission from biomass burning Total : 65 Tg / year

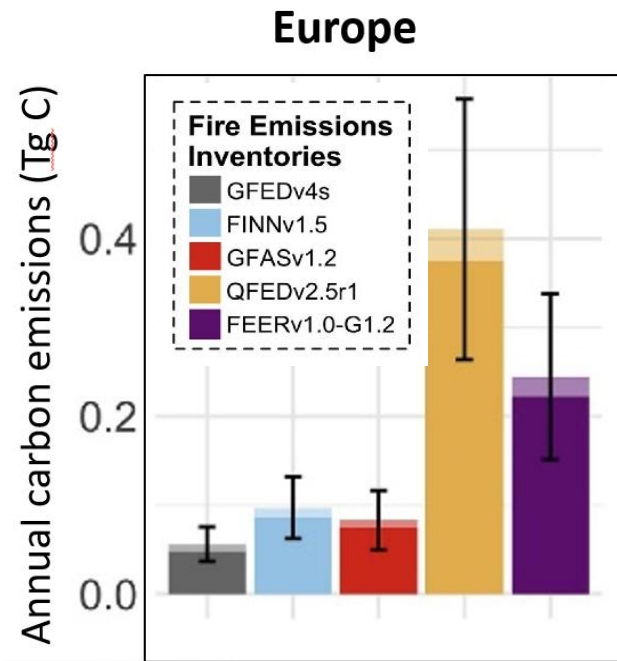


HCHO : high-yield product in isoprene oxidation



# Large differences between bottom-up inventories!

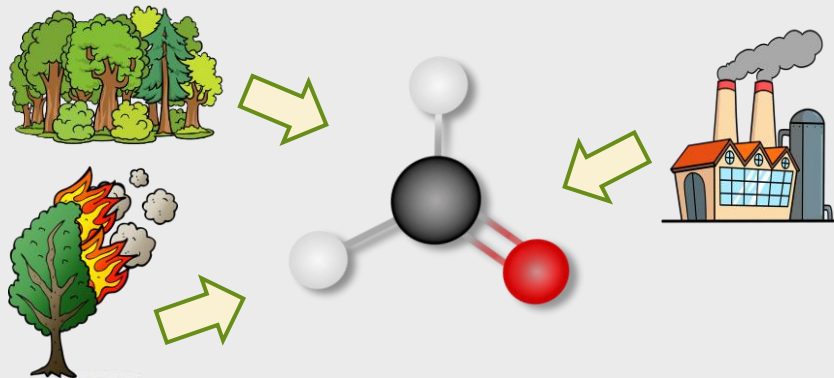
- Uncertainties due to detection of burnt area, FRP, emission factors, biome types, fuel consumption + difficulty to account for understory fires, peatland fires → hampers our understanding of fire impacts



- Factor of ~4 between global bottom-up estimates, larger differences at regional scale

BB datasets	Relies on
GFED4s	MODIS burnt area + active fires
FINN	MODIS active fire counts + active fires
GFAS	Assimilated MODIS FRP
FEER	As in GFAS, constrained by MODIS AOD
QFED	MODIS FRP + AOD
SEEDS	Top-down, based on HCHO data

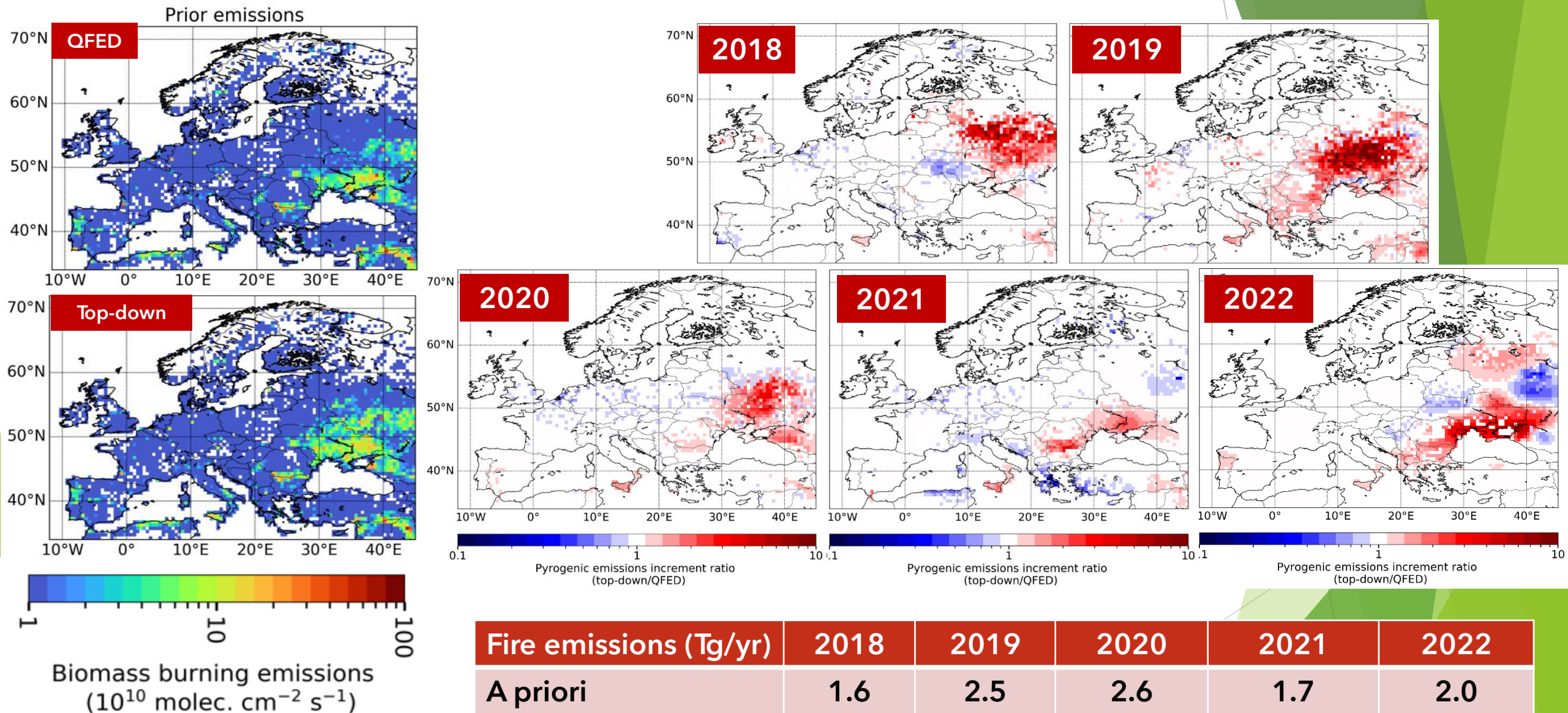
- Inventories perform differently depending on species, season, location



Is satellite HCHO an alternative way to constrain biomass burning emissions?



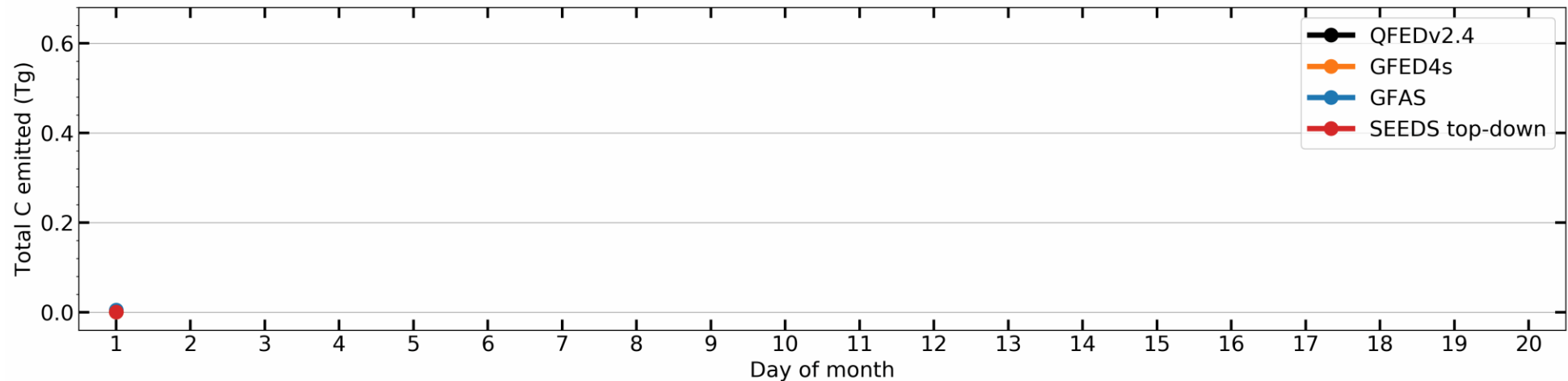
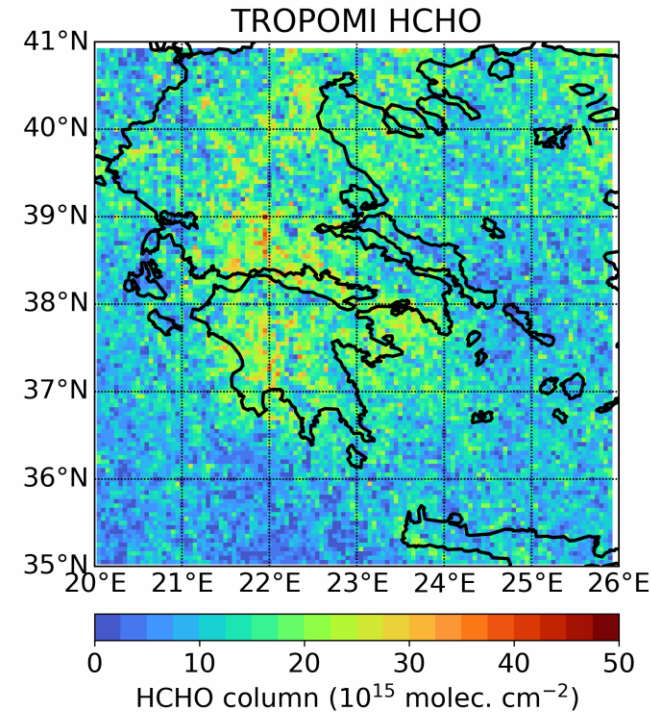
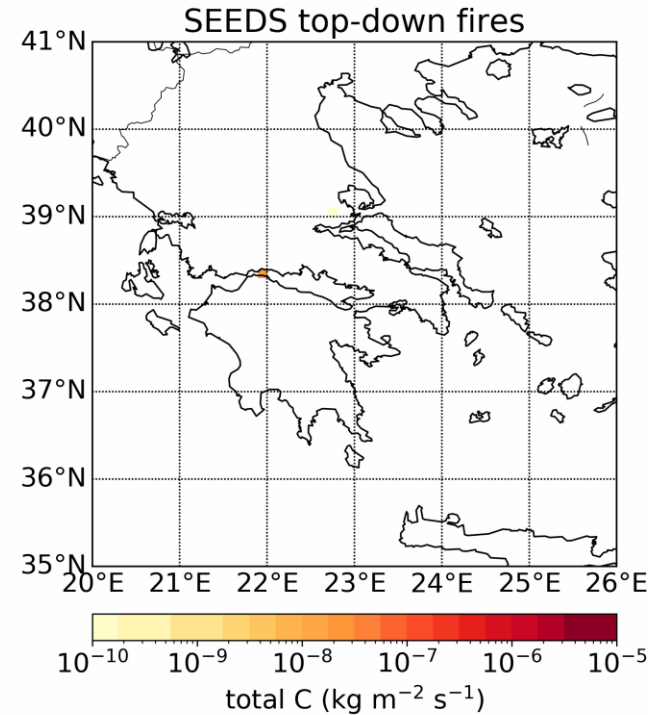
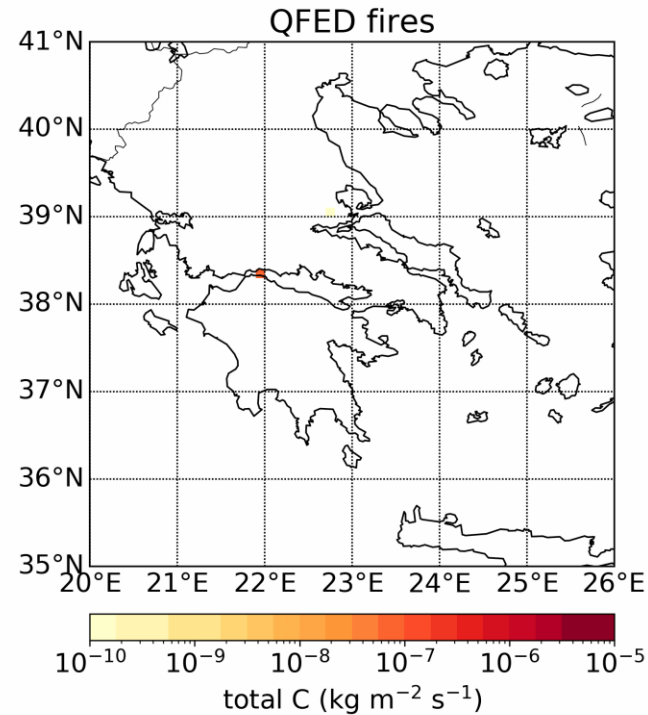
# Emission enhancements: average May-September



Fire emissions (Tg/yr)	2018	2019	2020	2021	2022
A priori	1.6	2.5	2.6	1.7	2.0
Top-down	2.1	3.5	2.9	1.7	1.8

# Top-down emissions during an extreme event

August 1 2021



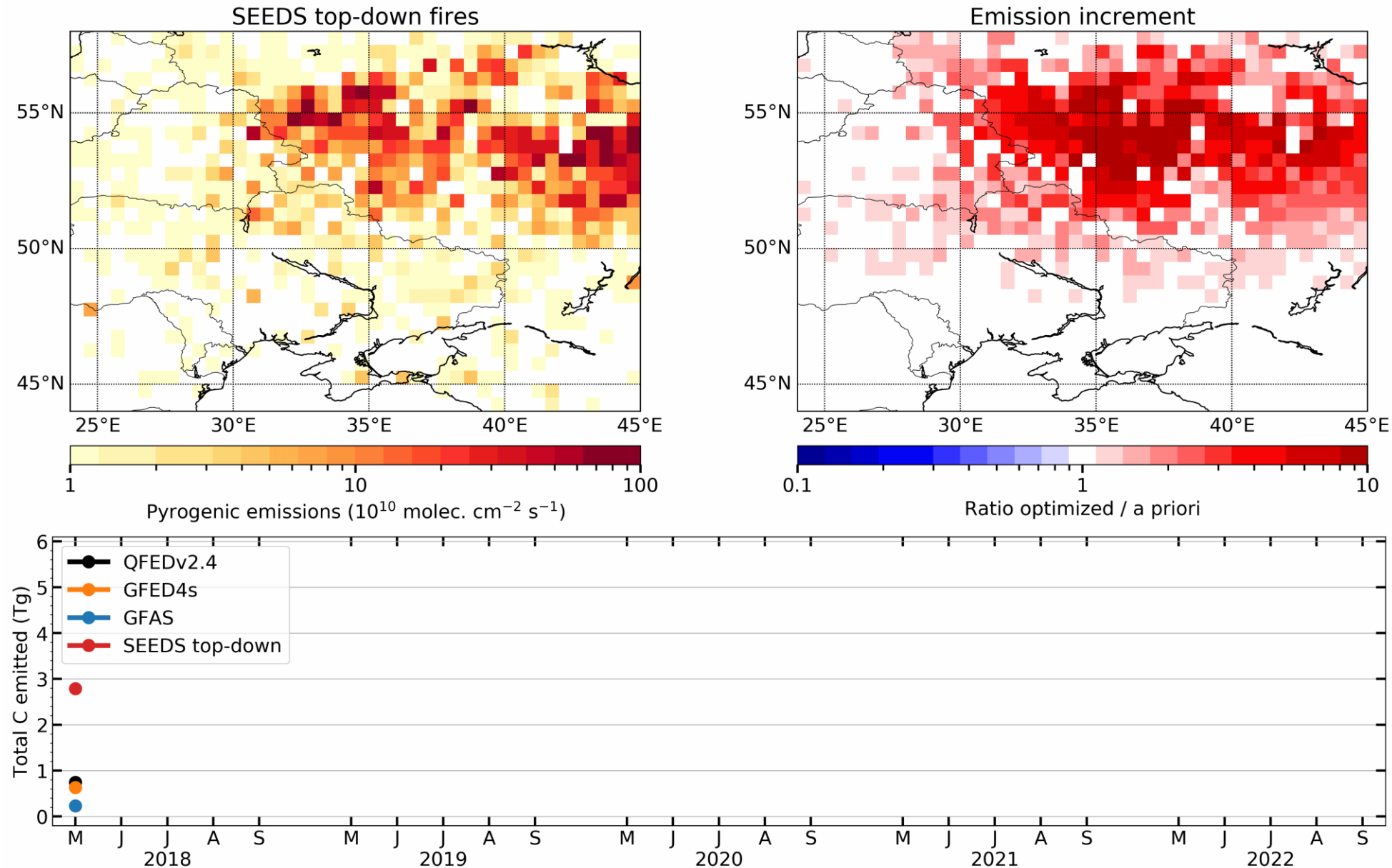
- Top-down emissions are lower than all inventories
- The peak on 6 Aug is well captured in all datasets, except for GFED
- The top-down peak is x2-3 lower than QFED/GFAS, could be due to the export of pollution due to strong winds



# Underestimated cropland burning in Ukraine/Russia

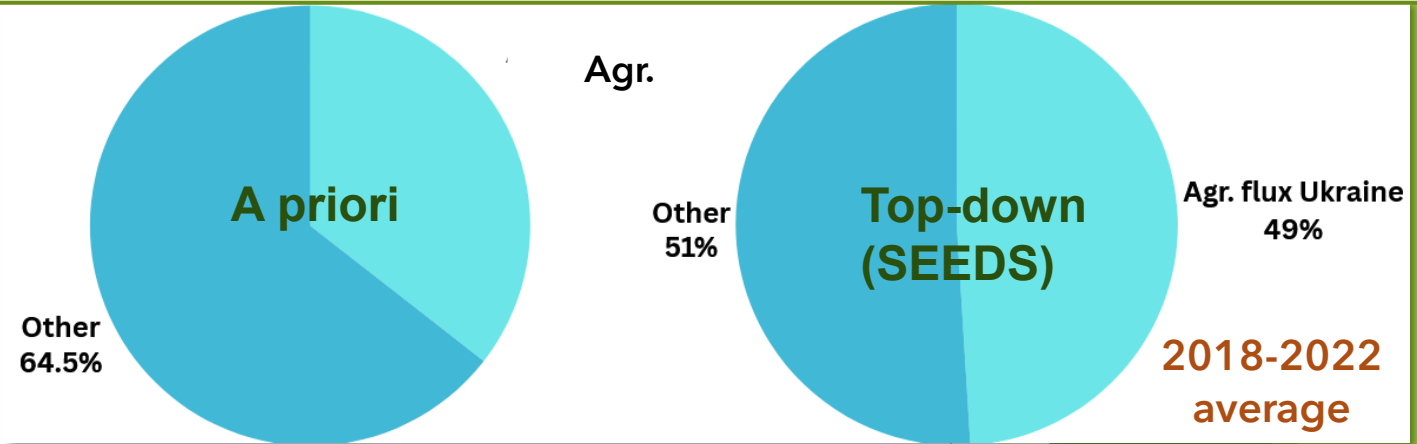
May 2018

- ✓ ~Half of Ukraine is cultivated area, 70% of land is dedicated to agricultural use
- ✓ Due to the small size of cropland fires, satellite burnt area is often underestimated
- ✓ SEEDS estimates are factor of 1.5-2 higher on average than QFED, GFAS estimates are the lowest



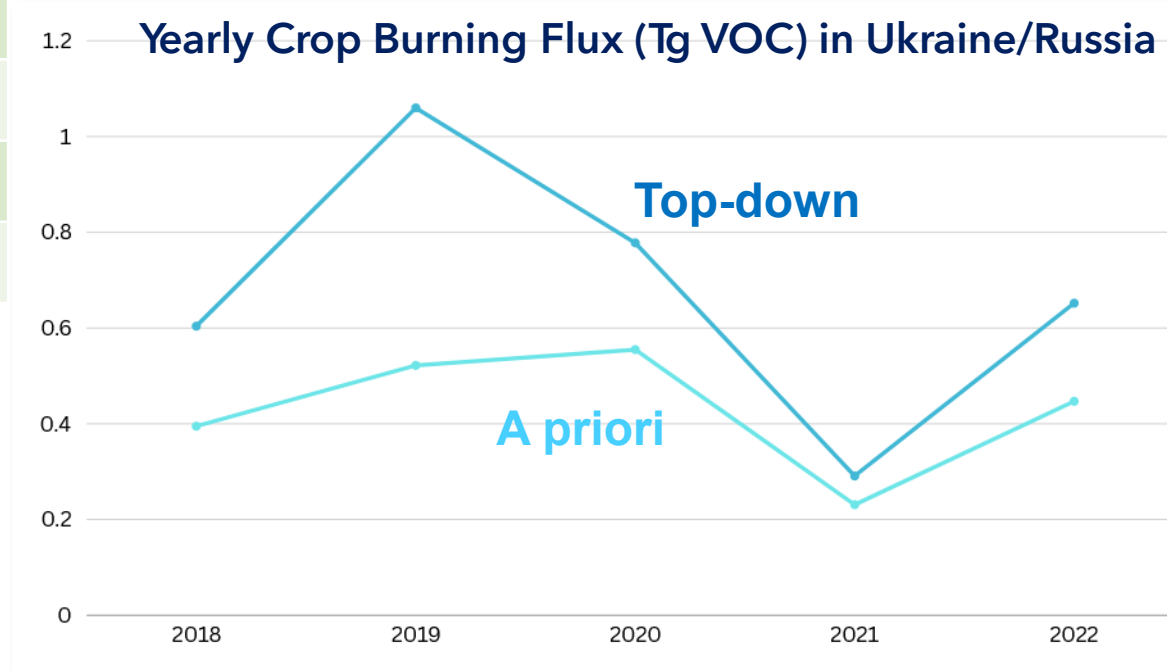
# Crop residue burning in Ukraine

The share of top-down crop residue burning in Ukraine accounts for half of the total flux estimate in the European domain; Increased wrt to the a priori



Ukraine/Russia fires	TgC (5-yr mean)
A priori (QFED)	5.9
GFED	3.7
GFAS	2.5
Top-down (SEEDS)	11.2

- ✓ Small fires are underrepresented in inventories, due to difficulties to map burnt area from satellites



- ✓ Top-down products offer an alternative estimate consistent with chemical observations, independent of fire proxies



# Biogenic BVOCs from the bottom-up perspective

- ✓ Natural emissions from vegetation are currently poorly constrained
- ✓ Large source of uncertainty in models

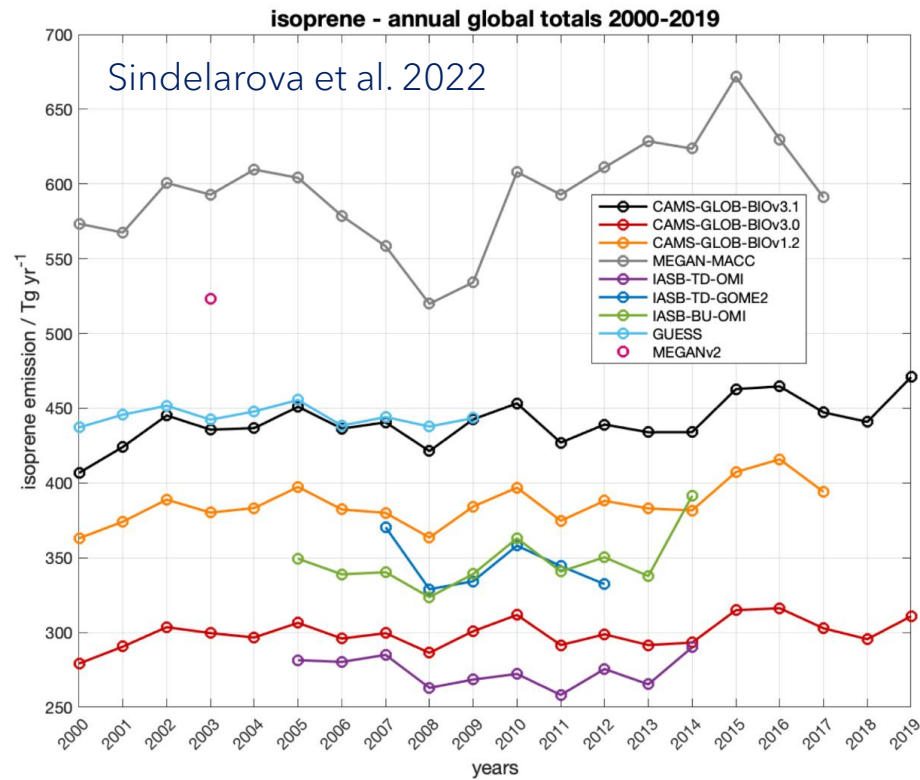
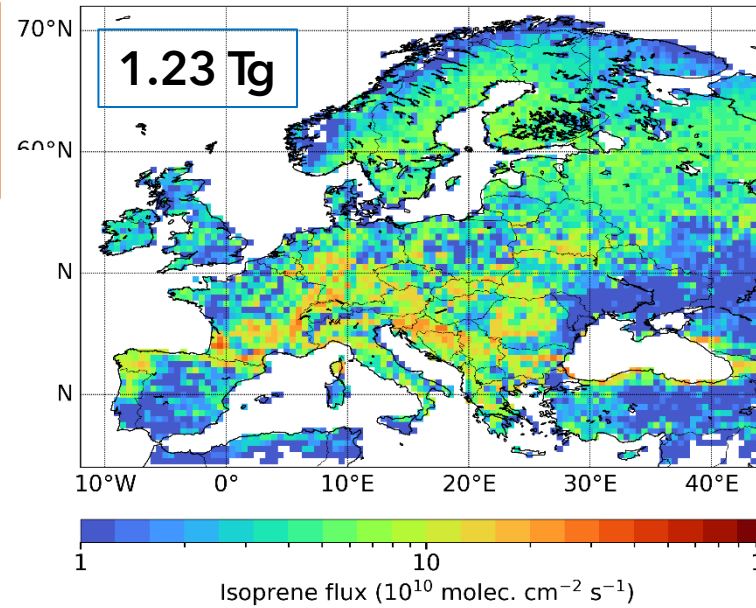
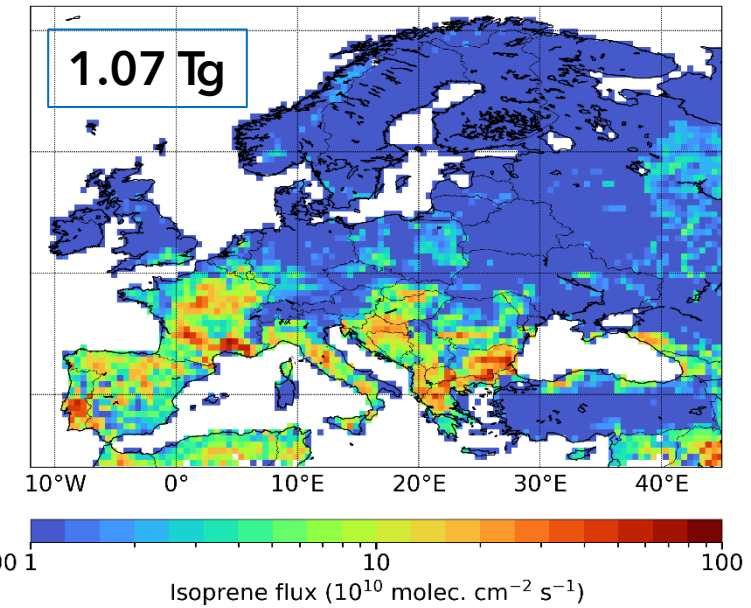


**Figure 7.** Comparison of isoprene global annual totals from CAMS-GLOB-BIOv3.1 (black), CAMS-GLOB-BIOv3.0 (red), CAMS-GLOB-BIOv1.2 (orange) and other available inventories within the 2000–2019 period.

MEGAN-SURFEX

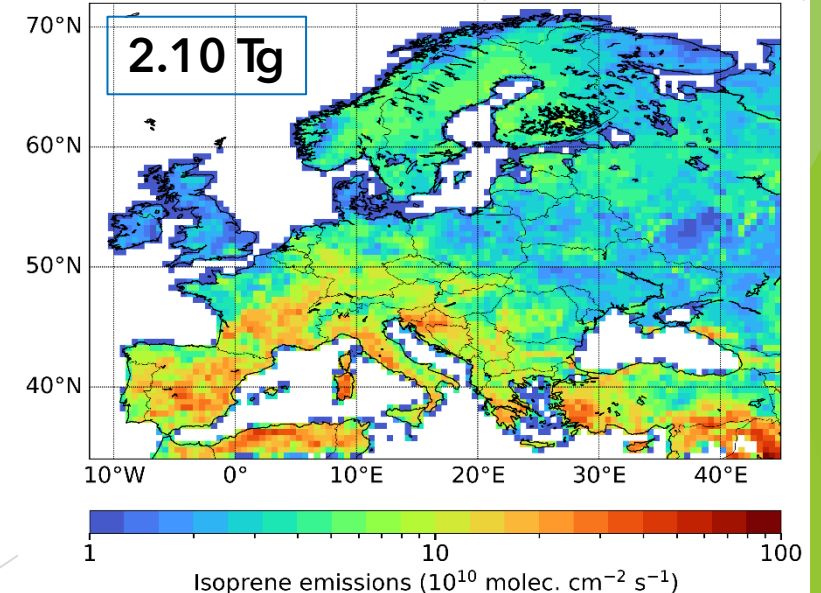


CAMS-GLOB-BIOv3.1 (Sindelarova et al. 2022)

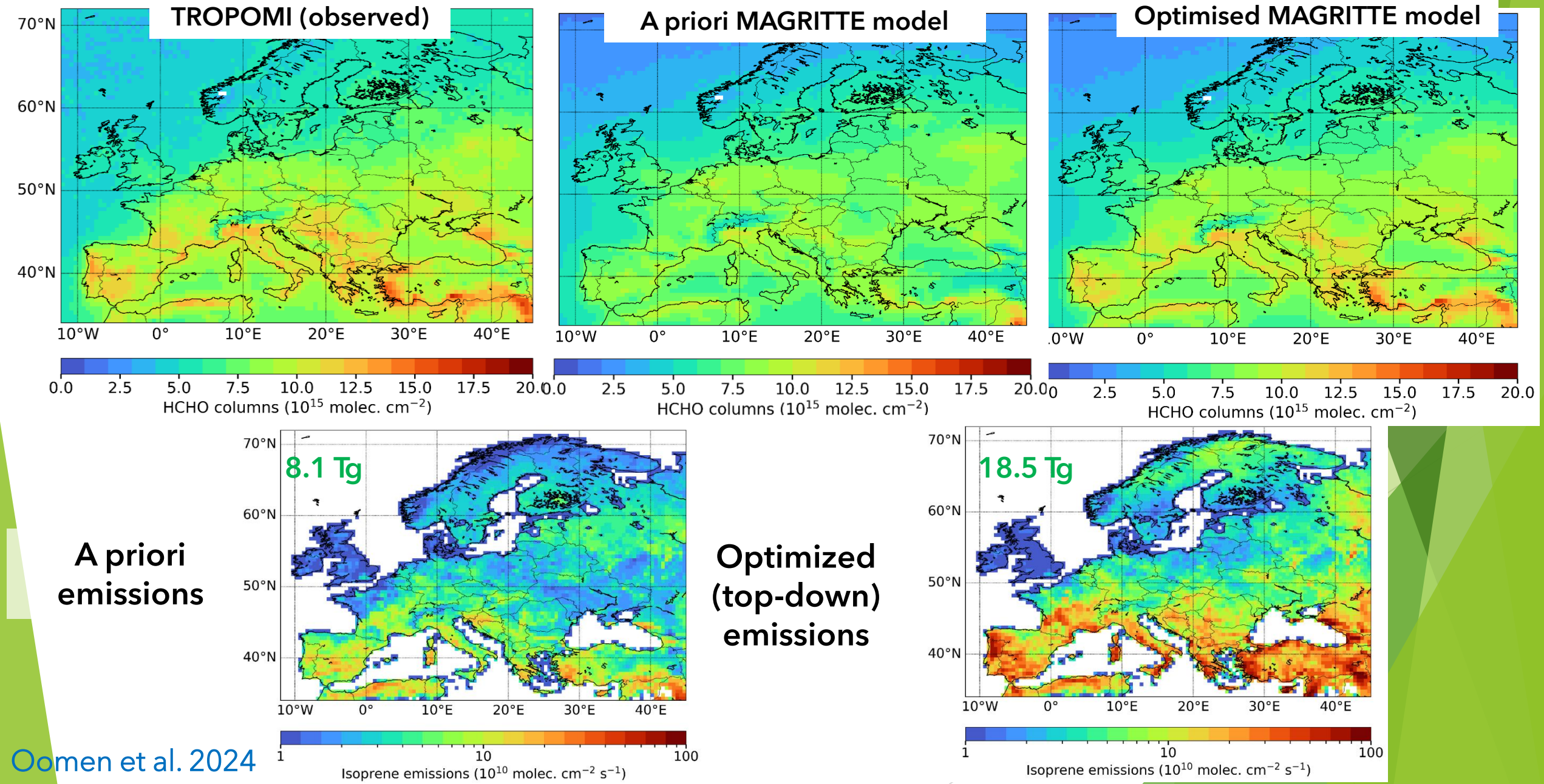


- ✓ In Europe, large differences found even among inventories built on the same emission model (MEGAN)

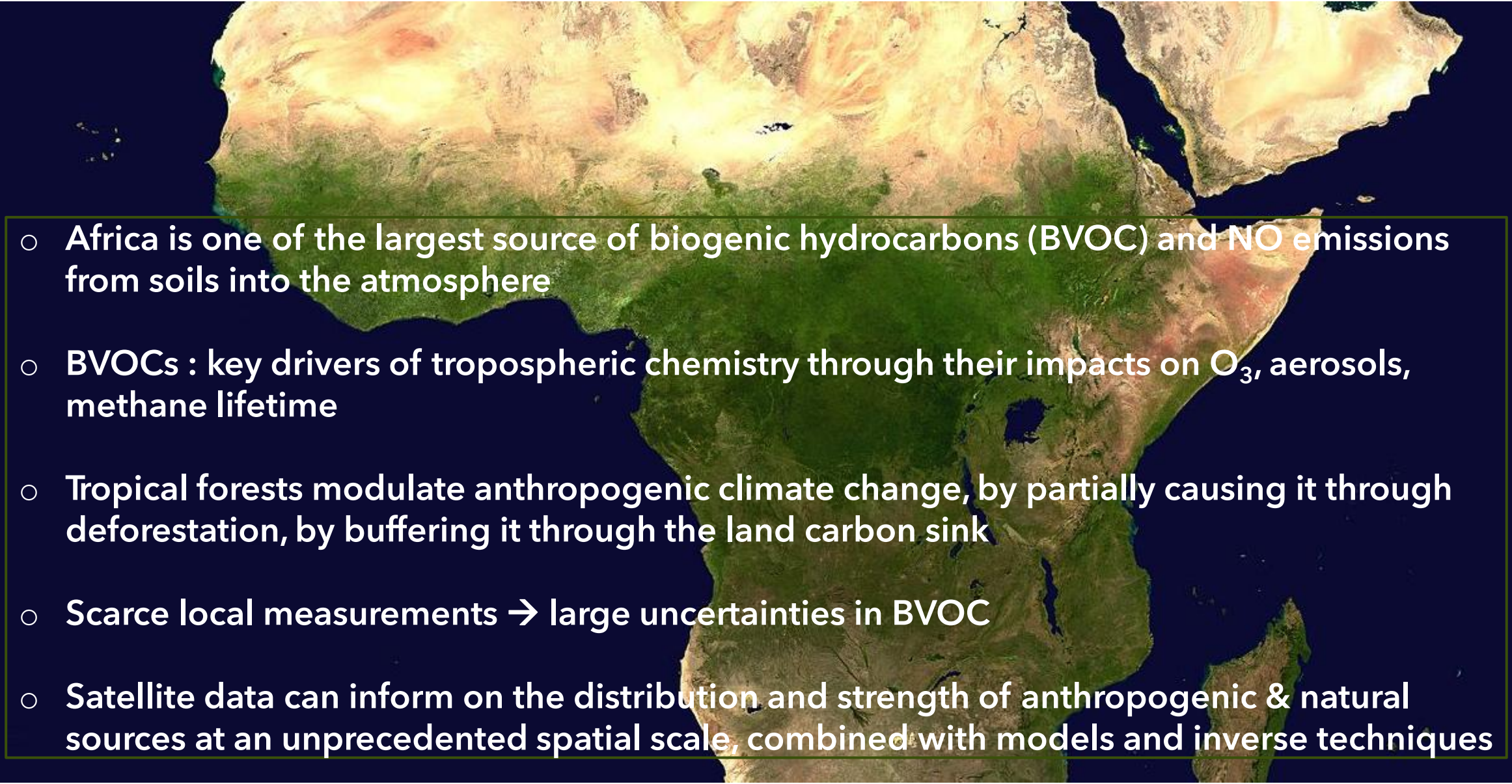
MEGAN-MOHYCAN (Stavrakou et al. 2018)



# ...and from the satellite perspective

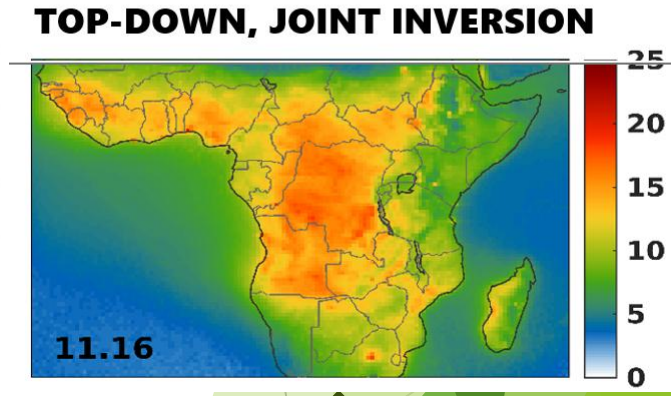
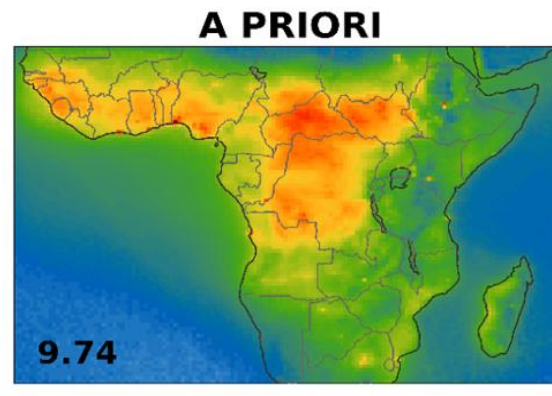
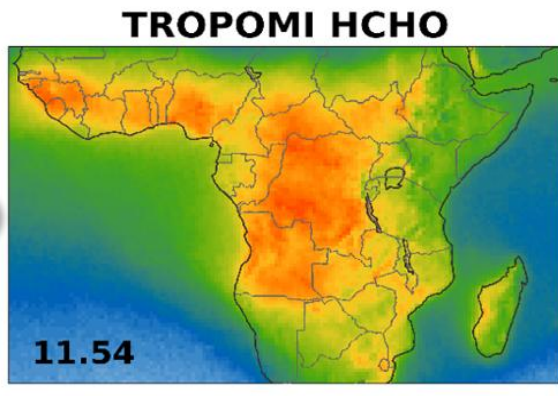
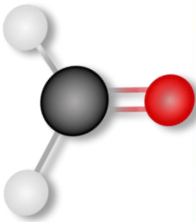
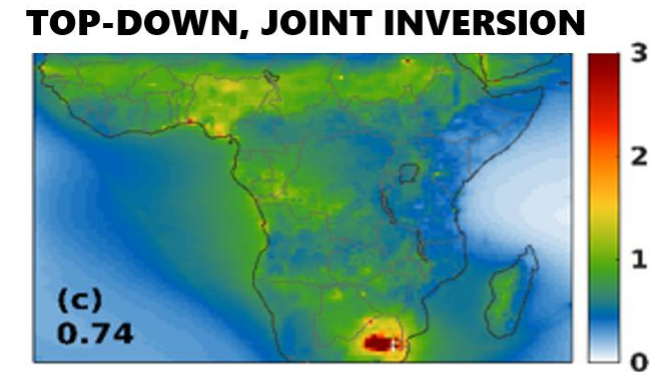
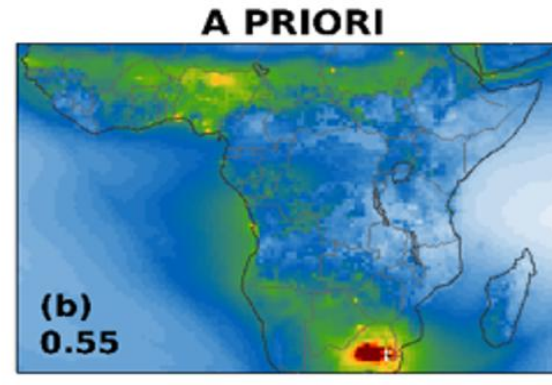
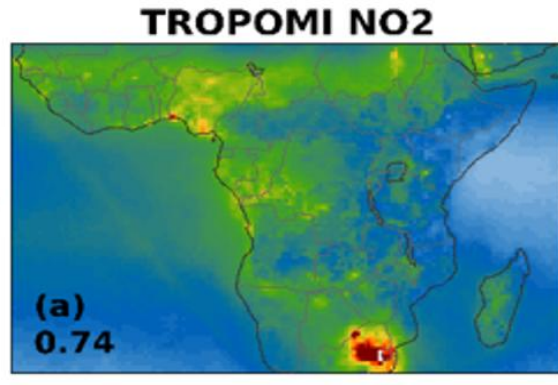
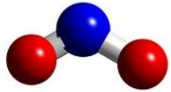




- 
- A satellite map of the African continent is shown in the background. The map uses a color scale where green represents dense vegetation (primarily tropical rainforests in Central Africa), yellow and orange represent semi-arid and arid regions (primarily in North and Southern Africa), and dark blue represents the surrounding oceans. The map is centered on the continent, showing its full extent from the Atlantic to the Indian Ocean.
- Africa is one of the largest source of biogenic hydrocarbons (BVOC) and NO emissions from soils into the atmosphere
  - BVOCs : key drivers of tropospheric chemistry through their impacts on  $O_3$ , aerosols, methane lifetime
  - Tropical forests modulate anthropogenic climate change, by partially causing it through deforestation, by buffering it through the land carbon sink
  - Scarce local measurements → large uncertainties in BVOC
  - Satellite data can inform on the distribution and strength of anthropogenic & natural sources at an unprecedented spatial scale, combined with models and inverse techniques

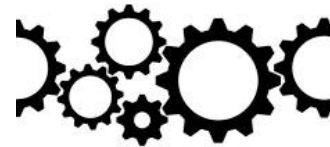


# Satellite NO<sub>2</sub> and HCHO data can inform about emission sources!



$10^{15} \text{ cm}^{-2}$

Opacka et al. 2025



Inverse methods

Very close agreement  
with observations  
achieved by significant  
emission changes





# Significant emission changes!

A PRIORI

TOP-DOWN

INCREMENT

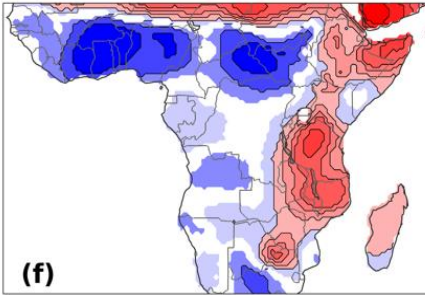
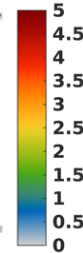
A PRIORI

TOP-DOWN

SOIL

1.9  
TgN

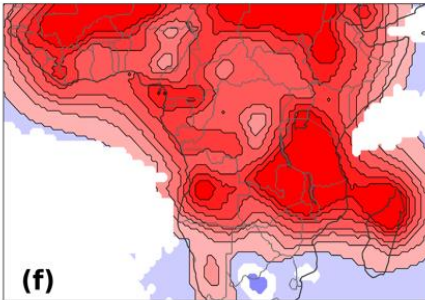
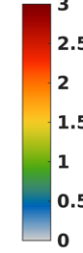
2.4  
TgN



LIGHTNING

0.5  
TgN

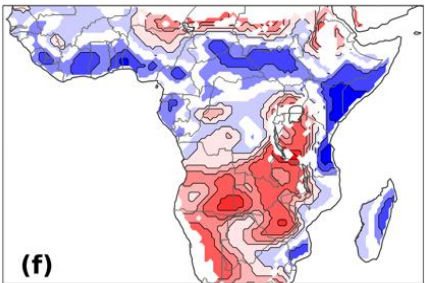
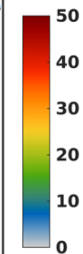
2.0  
TgN



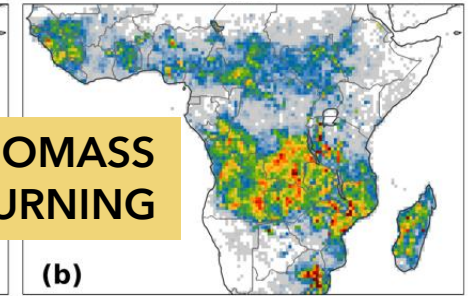
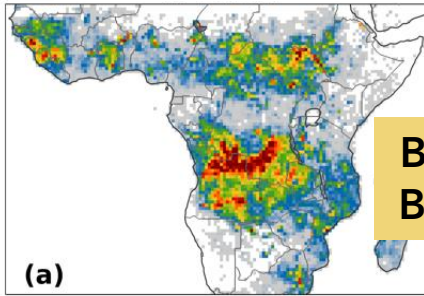
ISOPRENE

125 Tg

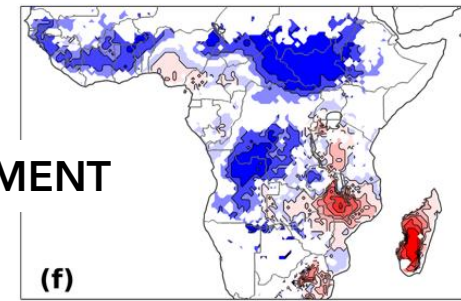
162\* Tg



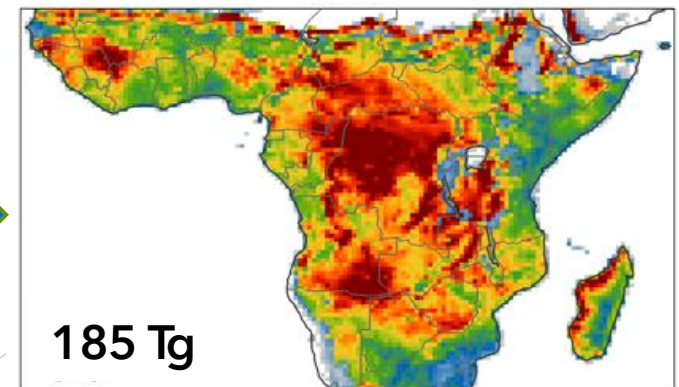
BIOMASS  
BURNING



INCREMENT



TOP-DOWN ISOPRENE,  
CONSTRAINED BY HCHO ONLY



\*185 Tg when  $\text{NO}_2$  is not used to  
constrain the inversion





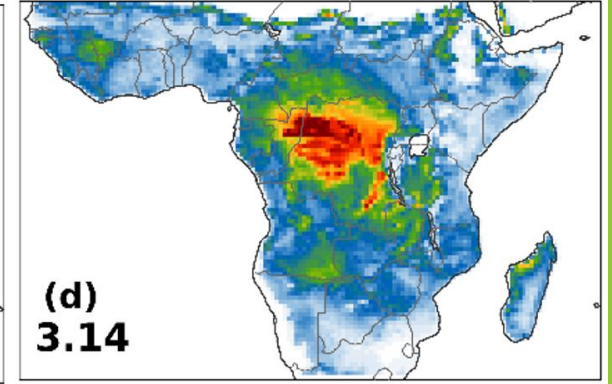
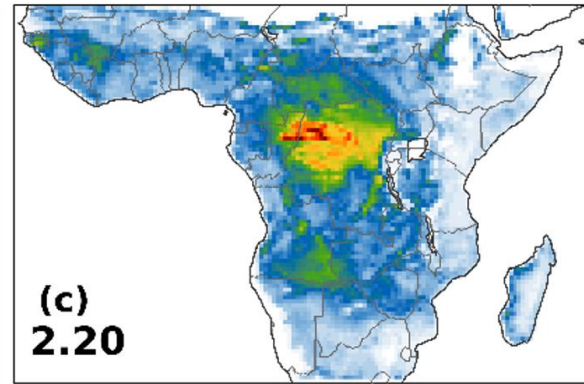
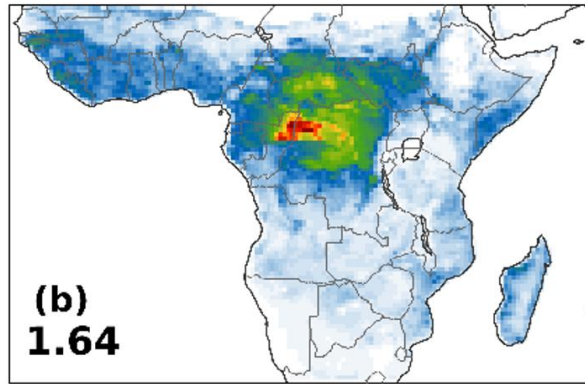
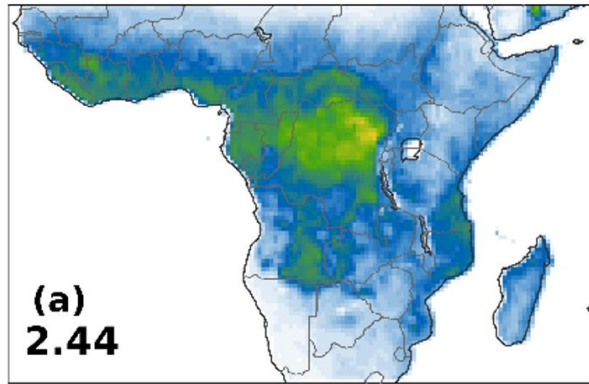
# Evaluation against CrIS isoprene columns

CrIS ISOPRENE  
COLUMNS

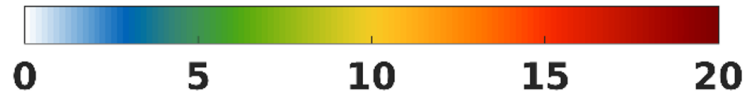
A PRIORI MODEL  
ISOPRENE COLUMNS

TOP-DOWN, JOINT  
INVERSION

TOP-DOWN, CONSTRAINED  
BY HCHO ONLY



Isoprene columns  
( $\times 10^{15}$  molec.  $\text{cm}^{-2}$ )



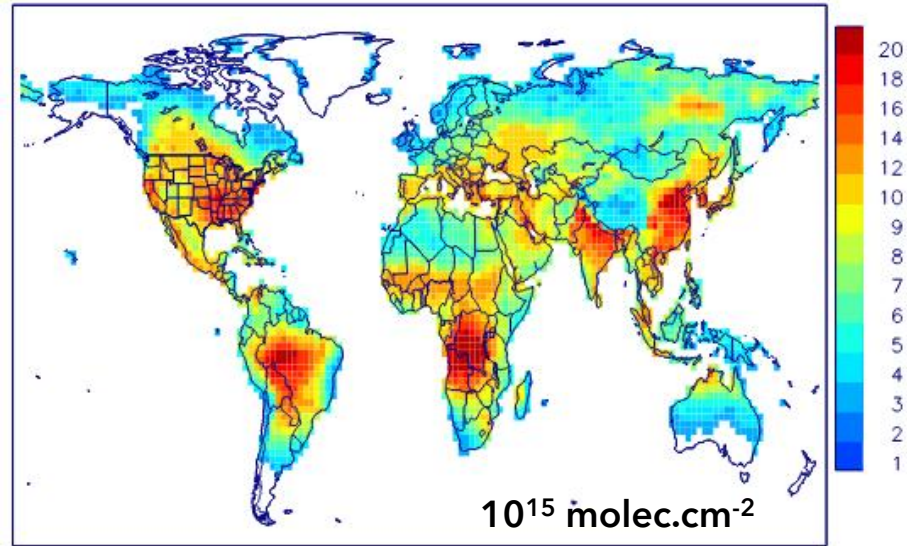
A priori spatial patterns are more contrasted than in the observations

Improved agreement with CrIS in the joint inversion (-33%  $\rightarrow$  -10%), improved spatial distribution

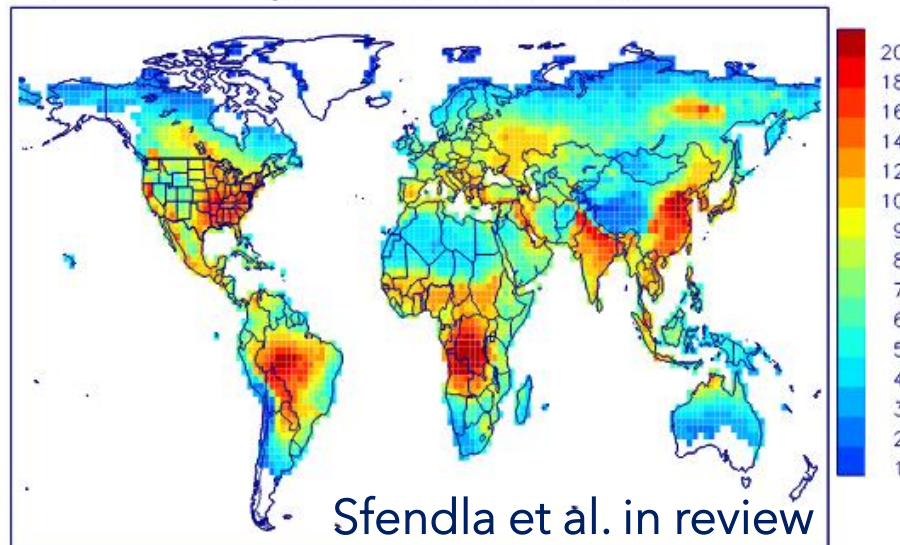
Compared to the joint inversion, increased columns by 40%. This is due to lower NO<sub>x</sub> fluxes, lower OH levels and longer isoprene lifetimes in HCHO-only inversion

# Inferred VOC emission fluxes on global scale using TROPOMI

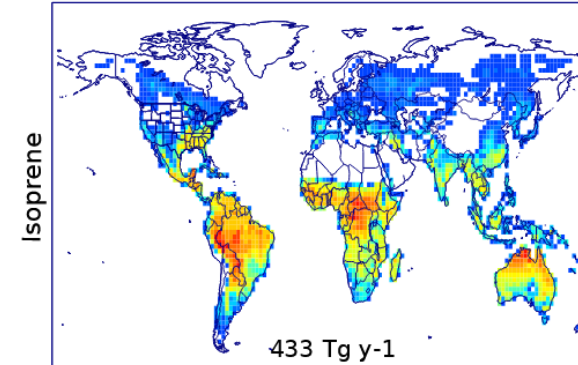
TROPOMI HCHO - JJA



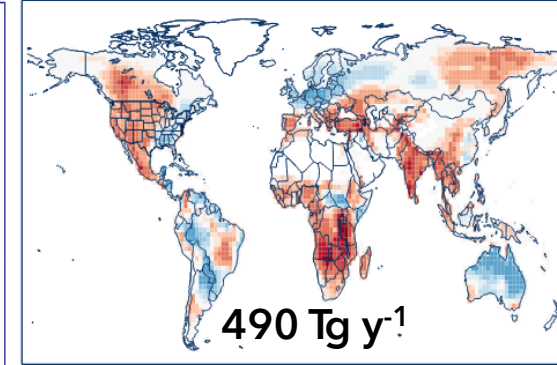
Optimized HCHO - JJA



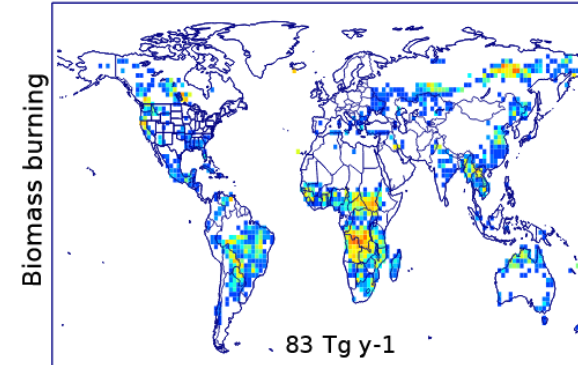
a. A priori emission flux (MEGAN)



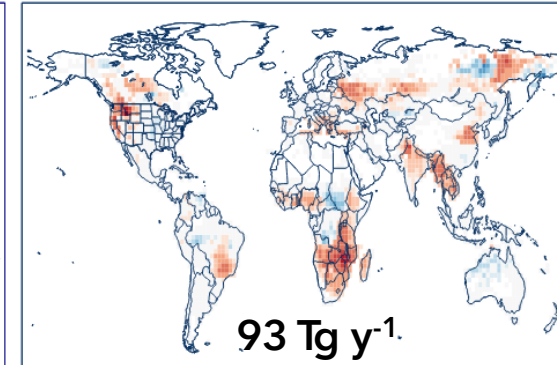
b. Optimized/a priori



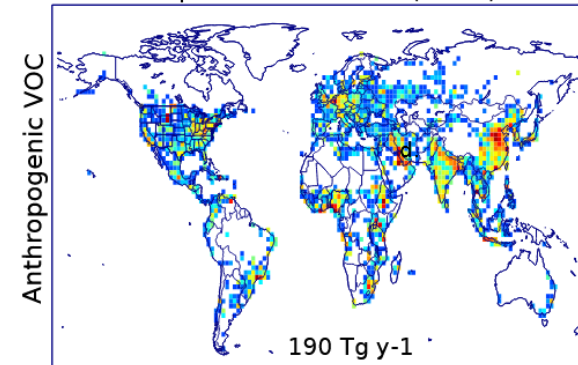
c. A priori emission flux (QFED)



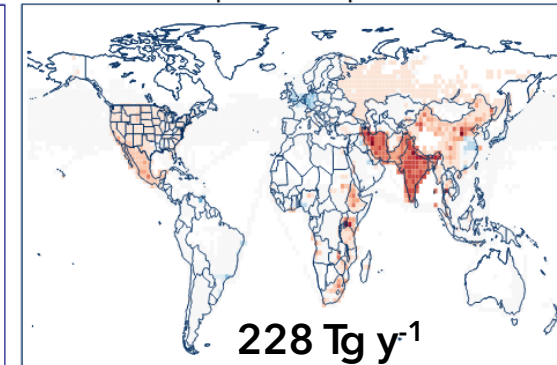
d. Optimized/a priori



e. A priori emission flux (CAM5)



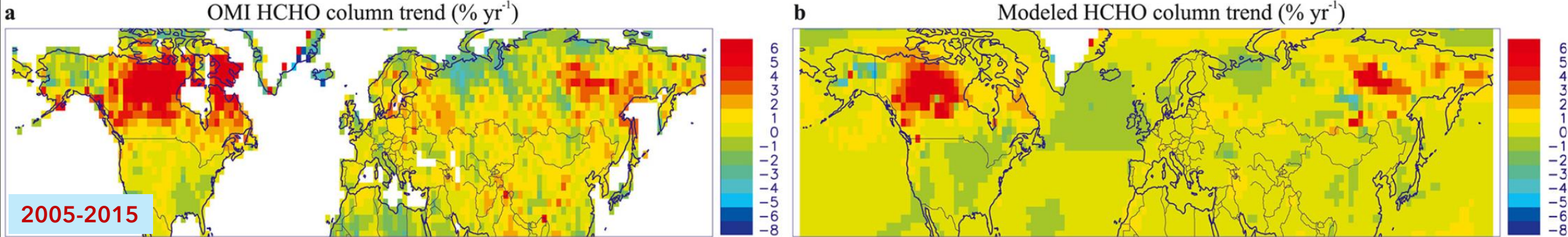
f. Optimized/a priori



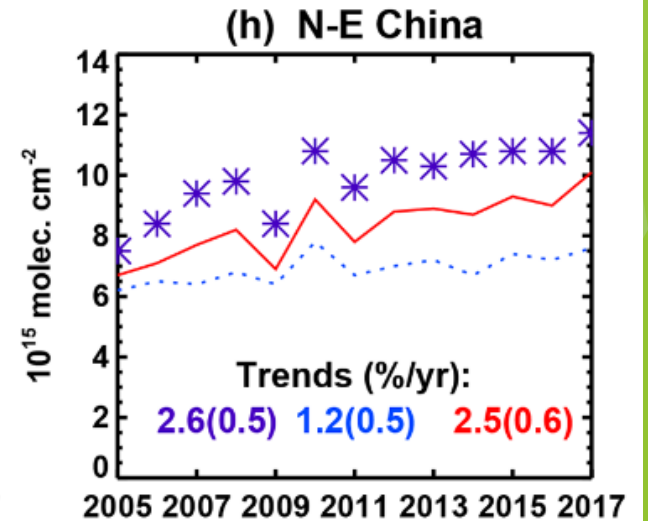
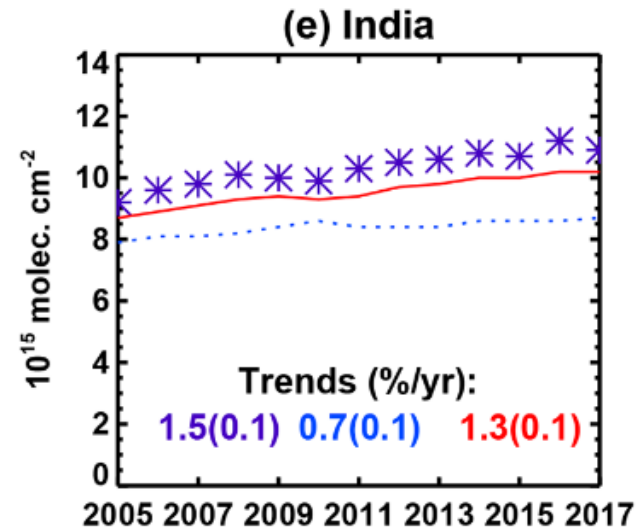
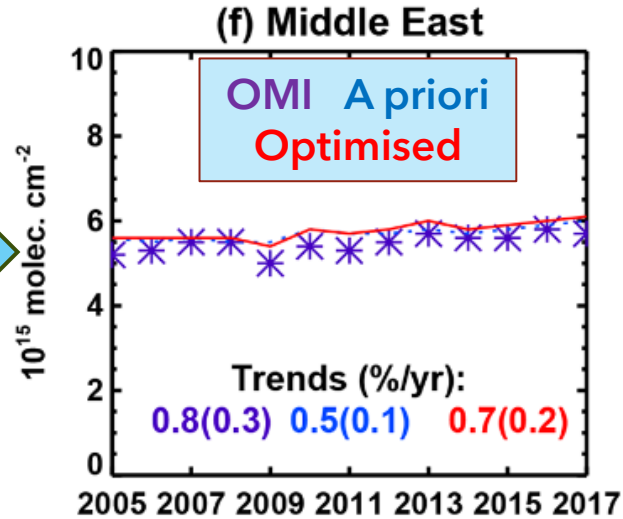


# Satellite-based trends

Clear evidence of a significant impact of climate variability over BVOC-dominated regions

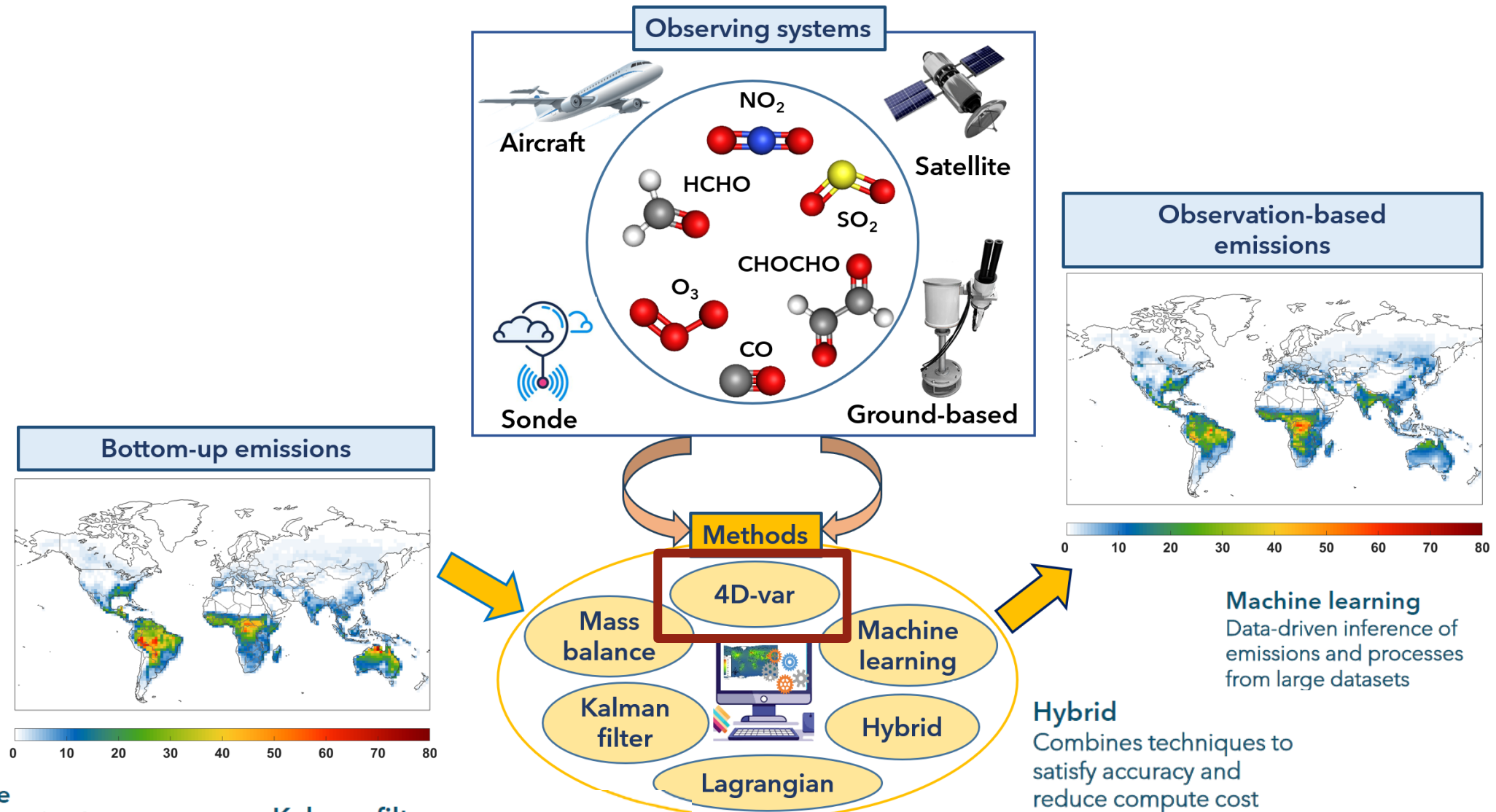


Inversion based  
on OMI HCHO  
over 2005-2017





# Other top-down approaches



## Mass-balance

Top-down approach inferring emissions from observed concentration changes assuming known transport and chemical changes

## Kalman filter

Sequential update scheme combining simulations with new observations; suited for real-time applications

## Lagrangian

Particle or trajectory modeling tracing plumes backward (sources) or forward (dispersion).

# Take-home messages

- Use of satellite data to learn about emission sources and their evolution, and to interpret the observed long-term satellite trends
- TROPOMI HCHO suggest increased fire fluxes from crop residue burning wrt bottom-up inventories and changes in spatial distribution of biogenic sources → geostationary observations offer promise to better determine these emissions
- Co-occurrence of sources (fires and enhanced vegetation emissions) during summertime makes it challenging to separate the sources
- Need for improved representation of pyrogenic and biogenic VOCs in models
- Inverse methods allow for a large array of applications & improved assessments of air quality (compounded by independent ground/satellite observations)